BNL-77899-2007-IR

Restoring a Damaged 16-Year-Old Insulating Polymer Concrete Dike Overlay: Repair Materials and Technologies

Toshifumi Sugama

September 2006

Energy Sciences and Technology Department/Energy Resources Division

Brookhaven National Laboratory
P.O. Box 5000
Upton, NY 11973-5000
www.bnl.gov

DISCLAIMER

Restoring a Damaged 16-year-old Insulating Polymer Concrete Dike Overlay: Repair Materials and Technologies

Final Report
(February 2002-July 2006)

by

Toshifumi Sugama
Energy Resources Division
Energy Sciences and Technology Department
Brookhaven National Laboratory
Upton, N.Y. 11973

For

Project Manager
Daniel D'Eletto
Principal Engineer
KeySpan Utility Services LLC
175 East Old Country Road
Hicksville, N.Y. 11801

September 2006

TABLE OF CONTENTS

Executive Summary

The objective of this program was to design and formulate organic polymer-based material systems suitable for repairing and restoring the overlay panels of insulating lightweight polymer concrete (ILPC) from the concrete floor and slope wall of a dike at KeySpan liquefied natural gas (LNG) facility in Greenpoint, Brooklyn, NY, just over sixteen years ago. It also included undertaking a small-scale field demonstration to ensure that the commercial repairing technologies were applicable to the designed and formulated materials.

The damage assessments of the16-year-old ILPC overlays consisting of a polyester polymer as the binder and lightweight multi cellular glass beads as thermally insulating aggregates revealed that the polyester binder had degraded due to exposure to ultraviolet (UV) radiation during those 16 years, which then promoted its saponification. Although the insulating property of ILPC remained in effect, the degradation of the polyester by the combination of UV radiation and saponification caused some degree of shrinkage of ILPC overlays, thereby resulting in the development of three different types of damage: 1) potholes created by spalling of the ILPC; 2) delamination of ILPC layers from the underlying concrete and their blisters; and, 3) evolution of map cracks and fissures. Type (1) damage was negligible; most of damages were types (2) and (3).

For dealing with the potholes as the type (1) damage, the material had to met the following eight criteria; 1) moderate plasticity, and an appropriate pot life of the ILPC slurry, 2) compressive strength of > 1500 psi, 3) density of < 50 Ib/ft^3 (< 0.8 g/cc), 4) flexure strength of > 600 psi, 5) thermal conductivity of < 0.13 Btu/hr-ft-°F, 6) excellent adherence to both the cement concrete and polyester-based old ILPC, 7) non-flammable, and 8) excellent resistance to UV radiation. We designed an epoxy-based insulating lightweight patching material system that met all these criteria. This system was comprised of 40.3wt% epoxy as the binder part A (ChemCo Systems, Inc), 17.3wt% polyamines catalyst as the binder part B (ChemCo Systems, Inc.), 31.0wt% aluminum silicate ceramic-shelled microspheres as the lightweight thermal insulator (PQ Corporation), 8.7wt% ammonium polyphosphate as the flame retardant (Exolite AP422, Clarian Corp.), 1.8wt% 2,4-di-tetriary-butylphenyl phosphate as the anti-oxidant (Naugard 524, Uniroyal Chemcial Corp.) and 0.9wt% aminopropylsilane triol as the

silane coupling agent (SIA 0608, Gelest Inc.). The system costs $17.24/ft^2 for a one-inch-deep pothole.

For damage types (2) and (3), our vacuuming-impregnation-coating finishing technology was adapted to rebind structurally the dormant and map cracks, and to hold the disrepair or broken pieces together; it also served to rejoin between the delaminated overlay and underlying concrete. Under the vacuum condition of -28 in.Hg, repairs were made with a wicking of 2wt% benzoyl peroxide (BPO)-catalyzed methyl methacrylate (MMA) monomer (Fox Industries Inc.) with a low viscosity of ~ 15 cps that permeated readily through the fine cracks of a less than 0.004 in. width and one in. depth existing in the ILPC layers. Nearly 20 minutes after the vacuuming-impregnation operation was completed, the MMA monomer that had penetrated in the cracks and fissures was cured, and had sealed these open spaces. Also, the permeated MMA satisfactory filled the interstices between the delaminated ILPC and underlying concrete, thereby rejoining between them. In this technology, the surfaces of repaired ILPCs and patched potholes were coated with an anti-flammable, UV resistant, and water-compatible material to protect the underlying ILPC overlays against fire, UV attack, cryogenic LNG spill, and more than 200 freeze-thaw cycles. We succeeded in modifying the commercial epoxy coating (Fox Industries Inc.) to meet all these criteria. The formula of the modified epoxy coating was 56.5wt% epoxy (FX-489 Part A), 28.2wt% epoxy (FX-489 part B), 12.7wt% ammonium polyphosphate anti-flammable reagent (Exolite AP422, Clarian Corp.), 1.6wt% 2,4-di-tetriary-butylphenyl phosphate anti-UV reagent (Naugard 524, Uniroyal Chemcial Corp.), and 1.0wt% aminopropylsilane triol silane coupling agent (SIA 0608, Gelest Inc.).

Based upon the information described above, our focus next shifted to conducting a small-field demonstration to ensure that the commercial repairing technology matched up for the designed and modified material systems could satisfactorily restore the damaged ILPC sloped wall. We evaluated the technical feasibility of the vacuuming-MMA impregnation-epoxy coating finishing method for the dormant- and map-cracked old ILPC overlay. No field demonstration was made for the patch repairing material system Nevertheless, on September 21-22, 2004, a field demonstration was carried out at the LNG facility in Greenpoint, Brooklyn NY, under the contract with Balvac Inc. An

ILPC sloped sidewall panel, 8-ft. in wide x 30-ft. in length was chosen for this test. The field demonstration by Balvac Inc. proved very impressive; after ~ 40 min. vacuuming operation, followed by ~ 12 min. impregnation of BPO-catalyzed MMA monomer, the spaces of micro-size cracks and delaminated areas in the sidewall panel were adequately filled. The MMA cured within ~ 12 hours after the vacuum-impregnating operation was completed. The surfaces of the MMA-impregnated ILPC panel then were coated with the anti-flammable, anti-UV, and water-comparable epoxy material. Two layers of coating were applied in this demonstration. The consistency of formulated epoxy coating was nearly perfect for lining it on the sloped wall's surfaces, reflecting the fabrication of uniform, continuous smooth coating layers without any dripping. A very promising result was obtained from the post-test analyses of the core samples taken from the repaired ILPC panel. The data revealed that most of the cracks and fissures were rebound by the impregnated MMA, which also bonded the delaminated ILPC to the underlying concrete. Some MMA even permeated into the underlying concrete to reinforce it. In fact, the tensile splitting test for this core sample demonstrated that although breakage took place in the concrete layer, ~ ½ in. thick concrete attached to the ILPC remained intact. In contrast, the non-repaired core sample was broken easily throughout the sample. Thus, this field demonstration strongly demonstrated that the vacuum-impregnating-coating finishing technology had a high potential for repairing the dormant and map cracks in the ILPC panel and reattaching the delaminated ILPC to the underlying concrete.

Based upon this field test, the estimated total cost of materials was ~ $ 920 for the 8-ft. wide x 30-ft. long ILPC panel. Of this total, ~ 65 % reflected the cost of the MMA used in the vacuuming-impregnating operation.

Despite a very promising result from the previous post-field test analyses, one year later, we visually observed the development of some cracks in the middle location of panel. The failure assessment disclosed that although the catalyzed MMA monomer, supplied from Fox Industries Inc. was fully permeated through the damaged ILPC, there was no curing of MMA in this particular area of the panel. Consequently, Balvac Inc. recommended that we evaluate a different-grade MMA made by Chemmasters Corp. to ensure that it cures satisfactorily.

For this new MMA system, contingent upon the field temperatures, BNL designed two formulations: One was 82 wt% MMA, 12 wt% catalyst, and 6 wt% promoter for use in an environment at 50°F; the other was 88 wt% MMA, 8 wt% catalyst, and 4 wt% promoter at 77°F.

Using the former formulation, a field demonstration was performed by Balvac Inc. in October 2005. As a result, significant progress was made from this field demonstration; namely, the new MMA allowed it to permeate adequately through the cracks in the damaged ILPC layer, and it was fully cured in the interspaces created by delaminating the ILPC from the underlying concrete. However, one serious concern raised from the post-field test analyses was the presence of irremovable water in the interspaces during a vacuuming operation, thereby causing the elastic behaviors of the cured MMA polymer. This elastic behavior was detrimental to the ultimate performance of MMA in linking strongly the delaminated ILPC to the underlying concrete. Thus, to eliminate any moisture trapped in the interspaces, there was a necessity of heating the surfaces of ILPC by a hot air-blowing heater before vacuuming.

Another critical issue to be addressed was the failure of the epoxy topcoating that protected the repaired ILPC against UV radiation and fire. The failure assessment showed that the copious map cracks and spallations of the coating layer were due to its thermal stresses by heat-cooling fatigue cycles in atmospheric environments. To deal with this problem, we recommended the development of the coatings, which will possess the following three critical properties: 1) Excellent thermal stability; 2) sufficient elasticity; and, 3) outstanding toughness. In addition, they must be resistant to UV, flame, and spilled LNG at the cryogenic temperature of -160°C (-260°F), and yet be well adherent to the underlying repaired dike.

1. Introduction

During 1985 and 1986, Brookhaven National Laboratory (BNL) developed an insulating lightweight polymer concrete (ILPC) as an insulation material and applied it to the surfaces of a cement concrete-based floor and sloped walls of a dike at a liquefied natural gas (LNG) facility in Greenpoint, Brooklyn, NY. The ILPC consisted of a polyester resin as the binder and lightweight multi cellular glass beads as the thermally insulated aggregate. In the event of a spill of LNG at its cryogenic temperature of –162°C (-260°F, atmospheric pressure), the major contribution of the ILPC overlay to the dike would be to reduce the rate of vaporization of any spilled LNG, thereby limiting the size of the flammable vapor cloud, and preventing it from traveling more than a few hundred feet from the top of the dike.

In June 2002, KeySpan Utility Services LLC and BNL visually inspected the 16-year-old ILPC panels to assess any damages and deteriorations. The assessment revealed that there were primarily three types of damages that needed to be addressed (Figure 1). First, spalling of the ILPC had created potholes; second, delamination of the ILPC had uplifted it from the underlying concrete; and, third, map cracks had developed in the ILPC's surfaces. All the types of damage were observed on the sloped sidewall panels. The failure mode of the floor overlay was due mainly to the last type of damage. Fragments of the damaged overlay were brought back to BNL to assess why such failure occurred. The results from the microprobe and spectroscopic analyses for these fragments were as follows:

1) The adherence of the ILPC to the underlying concrete was inadequate, causing the adhesive failure as shown by the loss of adhesion at the interfaces between the ILPC and the cement concrete;

2) The polyester resin was not completely cured as was evident from the emission of a strong odor from the uncured polyester resin when the fragments were broken.

3) The ester groups within the polyester had become transformed molecularly into carboxylate anion groups, $-COOR \rightarrow -COO^-$, representing the deterioration of the polyester polymer structure. We believed that this transformation was due to the combination of the ultraviolet (UV) radiation-catalyzed degradation, and the saponification of the polyester during its long-term exposure to an atmospheric

environment. Once its degradation had begun, a serious concern was the shrinkage of the overlay structure, promoting the delamination of ILPC from the underlying concrete. Further, an important question that needed to be addressed was whether the thermal insulation of these failed overlays was still as effective as they were. To answer this question, we examined the cross-sectional profile of the delaminated overlay by scanning electron microscopy (SEM). The SEM image revealed that the polymer matrix had tightly bound the lightweight insulating aggregates into a cohesive mass, seemingly suggesting that the ILPC retained its original effectiveness as the insulating material.

In 1996, BNL succeeded in developing a technology suitable for rehabilitating the damaged epoxy resin-based ILPC overlay of the LNG dike in Hicksville, NY. In this case, the epoxy resin was simply adopted as the repairing material. However, thus far, no work was undertaken at BNL in an attempt to restore the failed polyester resin-based ILPC.

2. Objectives of the Project

Based upon the information described above, an ideal method for restoring and rehabilitating the structural and surface integrity and for repairing large areas of map cracking or porosity was to rebind structurally the cracks and hold the disrepair or broken pieces together, and also was to rejoin between the delaminated overlay and underlying concrete. When the commercial polymeric repairing materials were applied to the failed overlay containing these three different types of damages, the materials were required to meet the following general criteria: 1) excellent resistance to UV radiation; 2) minimum shrinkage; 3) low surface tension so that they permeate easily into the micro-sized cracks; 4) good adherence to the polyester-based ILPC and the underlying cement concrete; 5) low thermal conductivity; 6) non-flammability or self-extinguishment; and, 6) high elastic modulus, flexure toughness and compressive strength.

The properties of the repairing materials and the repairing process technologies needed depended on the types of damage. The repairing technologies discussed here were based upon established and accepted methods and techniques currently used for the repairing conventional cement concrete structures and elements.

Patch Repair of Sloped Sidewall ILPC Panels

Although the areas to be patched are very small, we decided on formulating repair material systems consisting of a polymer matrix and a lightweight insulating aggregate. These systems were intended to be very stiff, so that they can be put in place with a hand tool. The surfaces of the placed material then were troweled to attain a smooth texture.

Repair of Dormant Cracks and Delaminated Areas in Sloped Sidewall

Catalyzed polymeric materials without any aggregate were used to deal with these areas; they were required to have moderate viscosity. Among the candidates for repairing technologies for these particular damages, we selected the vacuum-impregnation method that never had been used in repairing KeySpan's dikes in the past.

Sealing and Repair of Crazed and Map-cracked Floor Surfaces

A polymer-based sealant with low viscosity was used as a repair material for sealing crazed or map-cracked overlay surfaces. The sealant must possess a good wicking property to facilitate its permeation through the micro-sized cracks present in the superficial layer of the floor overlay. The vacuum-impregnation technology, the same as used in repairing the dormant cracks and delaminated areas, was also applied to restore the cracked floor surfaces.

Coating for Repaired Overlay Surfaces

In addition, we deposited an anti-UV and -flammable decoration liner on the repaired overlay surfaces to protect the underlying structure against fire, UV degradation, cryogenic LNG spill, and freeze-thaw cycles. As a bonus, this liner enhanced the appearance of the dike's overall surfaces. Multiple layers of liner are required to cover completely the repaired overlay surfaces. The coating was applied to the surfaces using brushes and rollers.

The work described in this final report began in January 2003 and was completed in January 2005. This work consisted of six major tasks:

Task A. Evaluation and Screening of Repairing Materials

Task B. Modification and Optimum Formulation of Repairing Material

Task C. Development of UV-and Flame-resistant Surface Coating

Task D. Small-scale Field Performance Tests

Task E. Cost Analysis of Materials

Task F. Preparation of Final Report

3. Experimental Procedure

3.1 Materials

Two commercial construction resins were used as the matrix for the patch repairing materials; epoxy (part A) and polyurea (part A), supplied from the ChemCo Systems, Inc. Incorporating two different hardeners cured these resins; polyamines (part B) for epoxy and amine blend (part B) for polyurea. For the epoxy, the ratio of the resin to hardener (part A: part B) in the mix was 2:1 by volume. For the polyurea resin to hardener mix (part A : part B), it was 1 : 1 by volume. Table 1 shows some physical and mechanical properties for these catalyzed resins and hardened polymers. As seen, the viscosity of catalyzed epoxy resin is lower by as much as 2.5 times than that of the catalyzed polyurea resin. Further, the tensile strength of the hardened epoxy polymer was more than twofold greater than that of the hardened polyurea. However, the polyurea polymer exhibited excellent elasticity; in fact, its elongation at break was 225 %, a value of ~ 3.8 times higher than that of the epoxy.

To enhance the insulating property of these polymer binders, PQ Corporation supplied hollow ceramic microspheres (Extendospheres SG) as a lightweight insulating filler. The bulk density of these microspheres was 0.4 g/cc. Figure 2 shows the SEM image and elemental analysis by energy-dispersive X-ray (EDX) for the Extendospheres SG.

A methyl methacrylate (MMA, FX-821) monomer with a low viscosity of ~ 15 cps was evaluated as a repairing material for delaminated and map-cracked areas using the vacuum-impregnation technology; the material was supplied by Fox Industries, Inc. The Benzoyl Peroxide (BPO) catalyst was added to MMA to cure it at room temperature.

An epoxy floor coating known by the trade name “FX-489”, supplied by Fox Industries, was used as the top coating on the repaired overlay surfaces. The FX-489 coating system consisted of two parts, a moisture-insensitive epoxy and an alkaline amine-based catalyst. With the volume proportions of 2 part epoxy to 1 part catalyst, the curing time of the coating at room temperature was ~ 40 min.

Three antioxidants, tetrakis[methylene (3.5,-di-t-butyl-4-hydroxyhydrocinmanate] methane (TMBHM), 4,4-bis (α, α-dimethylbenzl)diphenylamine (BDDA), and tris (2,4-di-tetriary-butylphenyl)phosphate (TTBH), supplied by Uniroyal Chemical, were used in an attempt to enhance the resistance of epoxy coating and patching materials to UV damage. These antioxidants, at 0.5, 1.0, and 2.0 % by weight of total amount of epoxy, were added to the catalyzed epoxy.

Clarian Corporation supplied two flame-retardants, Exolite AP 422 (ammonium polyphosphate) and Exolite AP 750 (nitrogen phosphorous compound). We evaluated their ability to retard the rate of flammability of the epoxy, and to suffocate its fire. Amounts of the flame-retardants up to 15% by weight of the catalyzed epoxy systems were incorporated into the systems.

In effort to improve the water-compatibleness of the epoxy coating, we evaluated two organic coupling agents supplied by Gelest Inc.; 3-aminoproply triethoxysilane (APTS) and aminopropylsilane triol (APST). The reason for selecting them was because the amino group in these coupling agents favorably reacts with the epoxy group in the coating, while the triethoxy and triol groups react directly with moisture to promote the linkages between the epoxy and the wet substrate.

4. Results and Discussions

4.1 Pothole-patching Materials

For successfully repairing the potholes created by the spallation of the old polyester ILPC, the material systems containing the pressure-resistant hollow micro-sized spheres as the insulating fillers must meet seven material criteria. Those criteria are addressed as follows; 1) moderate plasticity and an appropriate pot life of the slurry, 2) compressive strength of > 1500 psi, 3) density of < 50 Ib/ft^3 (< 0.8 g/cc), 4) flexure

strength of > 600 psi, 5) thermal conductivity of < 0.13 Btu/hr-ft-°F, and 6) excellent adherence to both the cement concrete and polyester-based old ILPC.

4.1.1. Formulations and Density of Patching Materials

Two resins, polyurea and epoxy, supplied from the ChemCo Systems, Inc. were used as binders of the patching materials. Ceramic microspheres (Extendosphere SG) with a density of 0.4 g/cc were used as the insulating filler. The formulations designed in this work for each binder are shown in Tables 2 and 3. They also include the density of patching materials made with these formulas. The data showed that the density for both the lightweight polyurea and epoxy polymer concrete (PC) patching materials depended on the amount of microspheres incorporated into them; namely, adding > 35 wt% microspheres was required to obtain a density of < 50 lb/ft^3. Regarding the slump properties of these lightweight resins, incorporating 55wt% microspheres into the epoxy achieved zero slump, but not in the polyurea (Figure 3). We observed some degree of slump for the 55wt% microsphere-incorporated polyurea slurry. However, when > 55wt% was added to these resins, it was very difficult to mix them thoroughly by hand.

4.1.2. Compressive Strength

Figure 4 shows the compressive strength of the lightweight PC specimens prepared by varying the amount of microspheres. As expected, the overall compressive strength for the PC specimens made with the elastomeric polyurea resin was much lower than for that of the epoxy-made PC specimens. The highest strength obtained from the elastic polyurea specimens was only 840 psi, which is ~ 2.4fold lower than that of the maximum strength of the epoxy specimens. The elastic behavior of polyurea PC specimen during compressive strength testing is showed in Figure 5. The data also revealed that strength tends to rise with an increasing amount of microspheres. However, beyond a certain amount, the strength of these specimens seems to decline. Since the criteria for the compressive strength is > 1500 psi, it was met by epoxy specimens containing 20 to 55wt% microspheres.

4.1.3. Flexure Strength

Figure 6 depicts the changes in flexure strength of the epoxy- and polyurea-based PC specimens as a function of microsphere content. As seen, all the specimens met the flexure strength criteria of > 600 psi. Outstanding strength was determined from the epoxy specimens. For instance, the 55wt% microsphere –incorporated epoxy specimens with a density of 41.88 lb/ft^3 had a flexure strength of 1350 psi, which was two-fold greater than that of the polyurea specimens made with the same amount of microspheres. A superior flexibility of the epoxy PC at its failure can be seen in Figure 7.

4.1.4. Thermal Conductivity

The C-Matic Guarded Heat Flow Meter (ASTM F433) was used to measure the thermal conductivity of 55wt% microsphere-filled epoxy and polyurea PC specimens (size, 2-in. diam. by 0.75-in. thickness). Since the cryogenic temperature of LNG is –260°F (-160°C), the thermal conductivity was measured over a wide range of temperature from – 260° to + 160°F (-162° to + 71°C). The results are illustrated in Figure 8. As seen, the value of thermal conductivity for both the epoxy and polyurea specimens tends to decline with a decreasing atmospheric temperature. Also, there was no significant difference in its value between them at the same atmospheric temperature. Both PC specimens had a very low thermal conductivity, ranging from 0.041 to 0.043 Btu/hr-ft-°F, at the cryogenic atmospheric temperature of –260°F. Since the thermal conductivity of insulating materials covering the underlying concrete's surface was required to be less than 0.13 Btu/hr-ft-°F, these PCs appear to act as an outstanding insulator against the spilling of LNG.

4.1.5. Adherence

One necessary property for the patch repairing materials is good adherence to both the damaged old ILPC overlay and the underlying cement concrete surfaces. Inadequate adhesion at the interfaces between the repairing materials and these adherends frequently causes failure of the patched materials because water penetrates into the spaces between the adherends and the patched materials. Thus, it is a very important to know how well the PC patching materials stick to these adherends.

To obtain this information, our attention focused on investigating the adherent properties of the PCs to the dry and wet surfaces of the damaged old polyester dike and the underlying cement concrete. In this work, the cement concrete specimens were prepared by mixing four components, 41.0 wt% Type I portland cement, 20.0wt% coarse aggregate, 20wt% sand, and 19.0w% water. The slurries were cast in 1-in. x 1-in. x 12-in. beam molds and then left for 24 hours to cure in air. The cured concrete specimens were removed from the molds, followed by immersing them for 7 days in water at 25°C. Afterwards the beam-shaped concrete adherends were cut in half with a diamond saw. One half of the beam was placed back into the same mold as previously used in making the specimens. To determine the extent of adhesion at interfaces between the old polyester-based ILPS overlay and the epoxy- and polyurea-based PCs, half inch thick fragments of the old ILPC were removed physically from the underlying dike concrete surfaces in the field and cut into 1-in. x 1-in squares. These squares of old ILPC then were joined by polyester adhesive to the cut surfaces of the concrete beams. The 55wt% microsphere-filled epoxy and polyurea slurries were poured in the half empty molds, and left for 2 days at 25°C to complete the curing of these PC slurries (Figure 9). Two different conditions, dry and wet, were employed to assess whether the PCs appropriately linked to the surfaces of the two adherends, the old ILPC and the cement concrete. The extent of adhesion at the joints was estimated by comparing the value of bond strength computed from the maximum bending load at the failure of the PC/adhered joints (Figure 10). Table 4 gives the results from these specimens. Also, the locus of the joint failure for the specimens after the bending test was visually examined to support these findings. The epoxy –based PC exhibited outstanding adherence to both the dry surfaces of the damaged old polyester–based ILPC overlay and the cement concrete, reflecting a great bond strength of 71.7 psi and 69.2 psi, respectively. The fracture surfaces for both specimens after testing disclosed that bond failure took place in the cement concrete adherends. Such a cohesive failure mode for the epoxy PC/old polyester ILPC/cement concrete joint system strongly demonstrated that the bond strengths at interfaces between the epoxy and old polyester and between the polyester and cement concrete were much greater than the strength of the cement concrete itself. The bond strength of the epoxy/wet polyester joints when applied to the aherends' wet surfaces was 36.4 psi,

corresponding to a decrease of 35% compared with that obtained from its dry surface. Visual observation of the failed specimens indicated that the locus of disbondment occurred at the interfaces between the epoxy and wet polyester adherend, which can be described as an adhesive failure mode. In contrast, a better adherence was observed at interfaces between the epoxy and the wet cement concrete, thereby resulting in good bond strength of 51.1 psi along with a mixed mode of cohesive and adhesive failures.

Unlike the epoxy, the adherence of the polyurea-based PC patching material to these adherends was poor, except for the dry cement concrete surface because of its high elastic property. As is evidence from the visual observation of bond failures at the polyurea/dry old polyester and polyurea/dry cement concrete joints, the cracks were initiated in the polyurea during the bending testing. Additionally, the polyurea did not adhere well to both the wet surfaces of old polyester ILPC and cement concrete; in fact, the bond strengths at such interfaces were only 13.5 psi and 10.1 psi, respectively.

4.2. Repair of Delaminated and Map-cracked Areas

4.2.1. Vacuuming-impregnation Sealing Technology

The vacuuming-impregnation technology has high potential for repairing the dormant cracks and delaminated areas as well as regions with map pattern-cracking because it can seal micro-sized cracks with appropriate repairing materials. Thus, the ideal sealing materials were required to possess a very low surface tension that allows them to wick and permeate easily into crazed and crack networks as narrow as 0.003 in. At the same time, the sealants permeating through the cracks had to forge a strong bond between the delaminated old ILPC and the underlying cement concrete. To achieve this goal, we used a methyl methacrylate (MMA) monomer with a low viscosity of ~ 15 cps. The first experiment focused on measuring the gel time of MMA containing the benzoyl peroxide (BPO) as a curing initiator at room temperature. Table 5 shows the changes in the gel time of MMA as a function of BPO content. Gel time was defined as the total elapsed time at the beginning of its gelling after mixing the two ingredients, MMA and BPO. Adding a 1.5wt% BPO to MMA resulted in a gel time of 28 min. As expected, the setting time of MMA became increasingly shorter as the amount of BPO was increased. For instant, after incorporating 5.0wt% BPO, the gel time was only 7-min. Nevertheless,

we decided that a gel time of 17 min generated by adding a 2.0wt% BPO allowed plenty of time for it to penetrate satisfactorily through the fractures and networks of cracks.

Our next experiment investigated how deep the MMA penetrated through the narrow cracks. Using a constant crack length of 0.2 in., the three different ranges in its crack's width were adopted: One, which represented the narrowest cracks ranged from a low of 0.003 in. to a high of 0.007 in.; the second ranged from 0.009 in. to 0.013 in.; the third covered the range 0.021-0.025 in. Since the damaged and cracked ILPC dikes was around 0.5 in., the polyester-based ILPC slurries were poured into 2 in. diam. x 0.5 in. high plastic molds to simulate 0.5 in thick ILPC dikes. The feeler gauges (Figure 11) of different widths then were embedded into the slurry to make defects that ranged in size from 0.003 in. to 0.025 in. (Figure 12, right). At the same time, the cement concrete specimens were prepared separately in molds, 2-in. diam. x 4-in. long, and dried them for 20 hours at 80°C for use as the dried underlying adherend (Figure 12, left). The cured disk-shaped ILPC including five defects was inserted in the mold containing the cement concrete, and pushed down to contact its surfaces. Afterward, the spaces between the defective topping ILPC disk and the mold were sealed using a silicon sealer to avoid any penetration of MMA through their spaces during its injection. The plastic mold containing the topping ILPC disk in conjunction with the cement concrete was placed in the vacuum-impregnation chamber (Figure 13). Holding them under a continuous vacuum at a -28 in.Hg for 10 min eliminated any air entrapped in the fractures in ILPC disk and in the interstices between the ILPC and underlying concrete. After this, a proper amount of 2wt% BPO-catalyzed MMA was injected through a funnel attached to the impregnating pipe on to the surface of defective ILPC (Figure 14). The impregnation of MMA was completed after ~ 20 second; approximately 20 min later, the MMA began to gel.

For the purpose of comparison, we also examined whether the MMA penetrates the cracks under non-vacuum conditions. Table 6 shows the results from our visual observations of the defective ILPC disk-to-cement concrete joints after impregnation of MMA with and without a vacuum. The vacuuming-impregnation technology gave very promising results. This technology allowed the MMA monomer to permeate through a fine crack less than 0.004 in. wide, and also to fill the interstices between the ILPC disk

and the underlying cement concrete. The latter plays a pivotal role in rejoining the delaminated, lifted ILPC layers with the underlying concrete because the MMA cured in this interstice offers strong coupling between them. In contrast, the major shortcoming of conventional non-vacuuming technology was a little or no penetration through cracks of < 0.013 in. wide, suggesting that this procedure could not assure the restoration of the delaminated ILPC layers.

4.2.2. Adherence

To obtain information on how strongly the permeated MMA adheres to both the polyester-based ILPC and cement concrete, our attention was focused on investigating the adherence of the MMA to dry and wet surfaces of the old polyester-based ILPC and cement concrete. The specimens for this adhesive test were prepared in the following sequence: First, the 1-in. x 1-in. x 6-in. cement concrete beam was placed in a 1-in. x 1-in. x 12-in. beam mold; second, the 1-in. x 1-in. x ½ -in. old ILPC was inserted into the beam mold at a distance of ~0.12 in. from the concrete beam to create an interstice; third, the epoxy PC slurry was cast into the remaining empty space in the mold to reinforce the old ILPC; and finally, the catalyzed MMA resin was poured into ~ 0.12 in. wide interstice between the cement concrete and old ILPC (Figure 16) and left for 48 hours before testing. Both dry and wet contact surfaces of two adherends, the old ILPC and cement concrete, were tested in evaluating the adherence of MMA to them. The extent of adhesion at the joints between the MMA repairing materials, and the old ILPC and concrete adherends was estimated by comparing the value of bond strength computed from the maximum bending load at the failure of the MMA/aherends joints. The bend-loading point was on the MMA adhesive located between the old PC and concrete. Table 7 shows the test results from these specimens. Also, the locus of the bond failure for the specimens after the bending test was visually examined to support these findings. For both old ILPC and cement concrete, the bond strength at the MMA-to-dry ILPC and-dry concrete joint was 44.2 psi, and the locus of disbandment was the mix mode of cohesive and adhesive failures. The mode of the former failure took place in the concrete, and the latter at the interfaces between the MMA and the concrete. In comparison with the bond strength at the epoxy-based PC pothole-patching materials/dry concrete joints described

earlier, this value was 25 % lower, suggesting that the adherence of epoxy to dry concrete was much greater than that of MMA. A very intriguing result was obtained from the MMA-to-wet old ILPC and -dry concrete joint system; namely, the interfacial bond strength of 39.8 psi fell only by 10 %, compared with that of the dry ILPC/MMA/ dry concrete joint system. Also, the failure mode was the same as that of the dry ILPC/MMA/ dry concrete joint. This finding strongly verified that although the old polyester ILPC was wet, MMA preferentially linked to its surfaces, rather than to those of the dry concrete. As expected, when the MMA came in contact with wet concrete, the bond strength developed at the interfaces between them was very poor, reflecting an adhesive failure at which the crack propagates from the interfaces. In fact, although the joint between the MMA and wet or dry ILPCs was sufficient, two joint systems, the dry ILPC /MMA/ wet concrete, and the wet ILPC/ MMA/ wet concrete, resulted in weak bond strengths of 22.8 and 24.9 psi, respectively.

4.3. Coating for Repaired Overlay Surfaces

In this task, considerable attention was concentrated on modifying and conferring advanced properties on the commercial epoxy floor coating known by the trade name "FX-489", supplied by Fox Industries, using flame retardants, UV-resistant reagents, and silane coupling agents.

4.3.1. Flame Retardants

Using two flame-retardants, Exolite AP 422 (ammonium polyphosphate) and Exolite AP 750 (nitrogen phosphorous compound), supplied by Clarian Corporation, our emphasis was directed toward assessing their effect on reducing the rate of flammability of the epoxy coating. We added flame retardants of 1, 2, 5, 10, and 15 % by weight of the total amount of the epoxy to the coating. A flammability test was performed on such modified epoxy samples, 5.08 in. long x 0.51 in. wide x 0.24 in. thick, according to ASTM D635, "Flammability of self-supporting plastics" (Figure 17). As evident from the findings (Table 8), both flame-retardants slowed down the rate of burning of the epoxy coating. The non-modified epoxy burnt out at the rate of 2.8 in./min (Figure 18). When 1 % Exolite AP422 was added, the rate of burning was reduced somewhat to 2.5

in./min. A further reduction to 1.8 in./min was obtained from 2 % Exolite AP422-modified samples. No significant difference in the effectiveness of flame retardation was observed with Exolite AP750; in fact, incorporating 2 % resulted in the same rate of burning as that of Exolite AP422 at the same concentration.

After adding amount more than 5wt% of these flame retardants, we observed a very promising result from samples modified with 15wt% Exolite AP 422, where there was no burning of epoxy (Figure 19). An amount of its 10wt% suffocated the flame about 100 sec after the fire was ignited in the epoxy, reflecting the retardant's self-extinguishing characteristics. However, the decrease in its concentration to 5wt% had no effect on suffocating the flame. In contrast, we noted that a lack of comparable effectiveness on self-extinguishing was observed from the epoxy modified with the Exolite AP 422; even if a high concentration of 15wt% was added, the samples burned until they suffocated themselves after ~69 sec. Therefore, we recommend using 15wt% Exolite AP 422 (ammonium polyphosphate) as a flame retardant for epoxy coating.

One concern about this recommendation was that such a respectable amount might impair the inherent mechanical and adherent properties of the original epoxy coating. In response to this important question, we examined the compressive (size, 2-in. diam. x 4-in. height cylinder) and flexural (1-in. x 1-in. x 12-in. long beam) strengths for the Exolite-filled epoxy specimens. Also, the adherence of the filled epoxy to the dry and wet MMA was estimated by the bond strength computed from the maximum bending load at the failure of the filled epoxy/MMA joints. In this test, the specimens were prepared in accordance with the following sequence: Firstly, the 1-in. x 1-in. x 6-in. dry or wet MMA beam was placed in the 1-in. x 1-in. x 12-in. long beam mold; secondly, the filled or non-filled epoxy slurry was cast into the remaining space in the mold to prepare epoxy/MMA joint specimens; and, finally, the joined specimens were left for 48 hour at room temperature before conducting the bend-loading testing.

Table 9 gives the compressive and flexure strengths for 0, 5, 10, and 20 wt% Exolite-filled epoxy specimens. Both the compressive and flexure strengths rose with an increasing content of the Exolite flame-retarding agent. Since this inorganic fine-powdered agent was insoluble in the epoxy resin, it is reasonable to rationalize that it distributed uniformly in the epoxy matrix so acting as reinforcement filler and

contributing to the improvement of mechanical properties of the epoxy. In fact, the compressive and flexure strengths of unfilled epoxy specimens increased ~34.5 % and ~39.3 % to 6543 psi and 1495 psi, respectively, as 15 wt% Exolite was added to them, strongly suggesting that there was no retrogressive effects on the mechanical properties from incorporating it.

Table 10 shows the bond strength at the joint between the Exolite-filled and unfilled epoxy, and dry or wet MMA. As expected, the adherence of epoxy to dry MMA surfaces was excellent, reflecting great bond strength of 280 psi. In contrast, the wet surface of MMA did not offer as effective a surface as did the dry one, as was reflected in a considerable reduction of bond strength to 99 psi, i.e., as much as 2.8-fold lower than that of the dry one. Thus, this epoxy seemed to be sensitive to moisture. No significant difference in adhesive behavior was observed from the 15wt% Exolite-filled epoxy; namely, its bond strength was 282 psi and 101 psi for dry and wet MMA surfaces, respectively. Exolite apparently had no effect in impairing the adherent behavior of the epoxy.

4.3.2 Ultraviolet (UV) radiation-resistant Regents

Organic polymers significantly absorb the UV radiation present in the solar spectral region reaching the earth's surface (wavelength, λ, > 300 nm). This process leads to the incorporation of oxygen into the their structure. Thus, the degree of UV damage in terms of photo degradation can be estimated by comparing relative numbers of carbonyl oxidative products formed in these polymer films after exposure to the portable high intensity UV lamp with a wavelength of 366 nm. The FT-IR was used to detect the carbonyl oxidative products. Photo oxidation means the cleavage of chemical bonds in a polymer structure, raising a major concern that cracking might develop.

Three antioxidants, tetrakis[methylene (3.5,-di-t-butyl-4-hydroxyhydrocinmanate] methane (TMBHM), 4,4-bis (α, α-dimethylbenzl)diphenylamine (BDDA), and tris (2,4-di-tetriary-butylphenyl)phosphate (TTBH), were supplied from the Uniroyal Chemical to inhibit UV damage of the epoxy coating. These antioxidants of 0.5, 1.0, and 2.0 % by weight of total amount of epoxy were added to the catalyzed epoxy. In preparing the UV exposure samples, we used the right-reflective aluminum panels, which were coated with

these antioxidant-modified epoxy resins by paintbrush. The coated panels were left for 24 hours at room temperature, and then heated them for 10 hours at 110°C to completely cure the resins. The coating films were exposed for 3 and 6 days to a portable high intensity UV lamp (Figure 20) for specular-reflectance FT-IR analysis. Particular attention was paid to detecting any carbonyl-related oxidation products formed in the epoxy during UV exposure. FT-IR analysis identifies the presence of carbonyl, C=O, oxidation products by the appearance of a wavenumber of near 1720 cm^{-1}.

Figure 21 gives the results of the FT-IR analysis for 1.0 % TMBHM-, BDDA-, and TTBH-modified epoxy samples after exposure for 6 days to UV. A high number of absorbance represents the incorporation of a large amount of oxygen into the epoxy during its exposure to UV, meaning that the epoxy underwent UV-caused oxidation damage. The data showed that the effectiveness of antioxidants in reducing the incorporation of oxygen depended on their species. The most effective one was TTBH, while TMBHM was identified as the second most effective one. In contrast, the BDDA did not offer as much oxidation protection as did two other antioxidants; in fact, BDDA enhanced the degree of oxidation of the epoxy.

Figure 22 shows the changes in absorbance at 1720 cm^{-1} of 0.5, 1.0, and 2.0wt% TTBH-modified epoxy samples as a function of UV exposure time for up to 6 days. For the unmodified epoxy denoted as the control, absorbance after exposure for 3 days rose 24 % to 0.24 compared with that before exposure. A further increase to 0.63 was evident in the 6 day-exposed samples, demonstrating that the epoxy progressively underwent UV-caused oxidation with an extended exposure time. Although the absorbance of all the TTBH-modified epoxy samples tended to rise with exposure time, the data clearly revealed that TTBH could abate the UV damage of the epoxy. With 0.5wt% of TTBH, an absorbance of 0.404 after 6-day exposure was tantamount to a reduction by as much as 35.7 % over that of the control sample exposed for the same time. An increase in concentration of TTBH further reduced absorbance, conferring enhanced resistance of the epoxy to UV. For instance, the absorbance of 0.159 obtained form 2.0wt% corresponded to a decrease of more than twice as much as that of 0.5wt%.

Figure 23 plots the absorbance versus UV exposure time for the TMBHM-modified epoxy samples. The results were similar to those from TTBH; an increase in the

amount of TMBHM improved performance in reducing the UV oxidation damage. In contrast, the BDDA anti-oxidant was not as effective as the other anti-oxidants. As seen in Figure 24, all of BDDA-modified epoxy samples underwent more UV damage than that of the control, except for the 2.0wt% BDDA sample after a 6-day exposure.

Thus, comparing the absorbance of 6-day-exposed epoxy samples, we ranked the effectiveness of anti-oxidants in mitigating UV damage in the following order: TTBH > TMBHM >> BDDA. Thus, we recommended employing TTBH as the UV-resistant additive for epoxy coating; the preferred amount was around 2% by weight of the total catalyzed epoxy.

4.3.3. Water-compatibleness

As described in 4.3.1. Flame Retardants, one issue to be addressed for the anti-flammable and-UV epoxy coating was its lower compatibility with water in terms of the coating having a poor affinity for moistened surfaces; in fact, when the epoxy was applied to the damp MMA's surface, the bond strength at the interfaces between them declined by nearly 3 times compared to that of the dry MMA's surface. This information strongly underscored the necessity of improving the ability of epoxy coating to adhere well to MMA's wet surface.

One way to achieving this goal was to modify the molecular structure of the epoxy with silane coupling agents, which provide adhesiveness to coatings, particularly for wet surfaces. We used two coupling agents from Gelest Inc., 3-aminoproply triethoxysilane (APTS) and aminopropylsilane triol (APST), because the amino groups in these coupling agents favorably react with the epoxy groups in the coating, while the triethoxy and triol groups react directly with moisture to promote linkages between the epoxy and wet substrate. The APTS and APST, respectively, of 0, 0.5, 1.0, and 3.0 % by weight of the total amount of the catalyzed epoxy were incorporated into the flame-retarded and UV-resistant epoxy resin. To estimate how well the APTS- and APST-modified epoxy coatings adhere to the MMA's wet surface, the bond strength at interfacial joint between them was determined. The specimens for the test were prepared in the following sequence: Firstly, the 1-in. x 1-in. x 6-in. wet MMA beam was placed in the 1-in. x 1-in. x 12-in. long beam mold; secondly, an unmodified or a modified epoxy

slurry containing 15wt% flame retardant and 2wt% UV resistant was cast into the remaining empty space in the mold to prepare the epoxy/MMA joint specimens; finally, the specimens were left for 48 hour at room temperature before conducting the bend-loading tests. The bond strength was computed from the maximum bending load at the failure of their joints.

Table 11 gives the bond strength at the joint between the modified and unmodified epoxy, and wet or dry MMA. As expected, the adherence of epoxy without these coupling agents to dry MMA surfaces was excellent as reflected in bond strength of 290 psi. In contrast, the adherence to the wet surface of MMA was not as effective as did the dry surface, causing a considerable reduction of bond strength to 99 psi, which was as much as 2.8-fold lower than that of the dry one. Thus, this epoxy appeared to be sensitive to moisture. When the APTS-modified epoxy was applied to MMA's wet surfaces, the data clearly demonstrated some restoration of the lost bonding strength. In fact, adding a 1wt% APTS led to developing a bond strength of 119 psi, corresponding to a 20 % improvement over that of the unmodified epoxy. Although the 3.0wt% APTS induced a further improvement of adhesive behavior, the extent of improvement was only 1.7 %, compared with that of the 1wt% addition.

In contrast, the APST coupling agent showed a better performance in improving the adherence of epoxy to wet MMA than did the APTS. For instance, with 0.5wt% coupling agent, the increase in bond strength above the unmodified epoxy rose by ~ 9 % and ~ 47 % to 108 psi and 145 psi for the APTS and APST, respectively. A further increase in content of the APST to 1.0wt% offered more improvement of epoxy's adherence; in fact, the resulting 179 psi bond strengths corresponded to an increase of 24%, over that of 0.5wt%. More interestingly, the locus of bond failure at the 1.0wt% APST-modified epoxy/wet MMA joints revealed a mixed mode of cohesive failure in the epoxy and adhesive failure at the interfaces. No cohesive failure modes were observed from the APTS-modified epoxy coatings, strongly emphasizing that its ability to improve the adherence of epoxy was far better than that of APTS. The data also showed that bond strength was not improved by adding APST to 3.0wt%. As a result, we recommend the addition of 1.0wt% APST to the epoxy coating.

4.4. Durability of Repaired ILPC

4.4.1. Cryogenic Temperature

Assuming that a catastrophic failure of the liquefied natural gas (LNG) tank took place at its storage site, and LNG at the cryogenic temperature of -160°C (-260°F) was spilled over the repaired ILPC dike surfaces, an emphasis focused on assessing whether the repaired dike is vulnerable to the attack of such an extremely low temperature fluid. To obtain this information, we employed liquid nitrogen (LN) at the cryogenic temperature of –209.9°C (-345.8°F), which is ~ 50°C (~ 86°F) lower than that of LNG.

Since the lifted and delaminated ILPC dikes would be repaired by a two-step route involving MMA impregnation, and a non-flammable, anti-oxidant epoxy overlay, the principal structure of repaired ILPC dike would consist of four different layers: 1) Cement concrete as an underlying layer; 2) a penetrated MMA layer adhering to the underlying concrete; 3) an MMA-impregnated old-failed ILPC layer; and, 4) an epoxy top coating layer. Thus, we used samples made under the four different conditions (see Table 12) for the LN spilling test. Table 13 gives the formulation for each of concrete, impregnating, and coating materials. The samples were prepared in a cylindrical mold (3.0 in. diam. x 3.5 in. high), and then were placed in a Styrofoam insulating box (Figure 25). The LN was directly spilled over the coatings' surfaces. As soon as LN came in contact with the warm coatings' surfaces, an oxygen deficient vapor cloud rapidly formed, thereby obscuring all visibility (Figure 26). About 3 min after spilling, the vapor cloud was dispersed by the prevailing air flow (Figure 27). Most of the ~ one inch deep LN pool over the coatings was dissipated within 10 min. The samples were left for 24 hours at room temperature before visually observing their surface and cross-sectional profiles. As shown (Figure 28), neither delaminations nor blisters were seen on the coating's surfaces of all the samples, underscoring that although the surfaces of ILPC dike repaired with MMA were wet, the BNL-formulated epoxy coating strongly adhered to the wet MMA. More importantly, the entire structure remained intact. The cryogenic LN did not cause any separation and segregation of the layers (Figure 29). From this encouraging result, we believe that the ILPC dikes repaired with this technology will withstand a LNG spill.

4.4.2. Freeze-thaw Cycling

Although the repaired ILPC dike withstood a cryogenic temperature, another concern to be addressed was its freeze-thaw durability; in particular, the bond durability at the interfacial joints between the underlying concrete and MMA-impregnated old ILPC dike and between the MMA-impregnated ILPC dike and the epoxy top coating. In response to this question, we prepared the specimens similar to those made for the previous LN spilling test. The specimens were submerged in water in the freeze-thaw cycling chamber as per ASTM C666 Test, and were subjected to a series of 6 cycles per 24 hours period based upon a one cycling temperature between 0 and 50°F. Specimens were removed from the freeze-thaw chamber after 10, 20, 30, 50, 100, and 200 cycles, and then their appearances were observed to obtain information on whether failure and disbandment at the joints had taken place. After 200 cycles, all specimens exhibited no changes in appearance; reflecting no delamination of the top coating layer, despite the wet concrete and wet MMA-impregnated ILPC in this joint system (see the sample I.D. 4 in Table 12). Further, we saw no separation at any joints on examining the cross-sectional profile (Figure 30), confirming the excellent durability of these bonded joints in the 200 freeze-thawing cycles.

4.5. Small-scale Field Demonstration

Since the areas requiring patch repairing is very small, our focus in this small-scale field test concentrated on evaluating the technical feasibility of the vacuuming-impregnation-coating repairing method for dormant- and map-crack areas.

On September 21-22, 2004, a field demonstration was performed at KeySpan liquefied natural gas (LNG) facility in Greenpoint, Brooklyn NY, under contract with the Balvac Inc. A sloped sidewall panel, 8-ft. in wide x 30-ft. in length (Figure 31), was selected for this test. There were no large holes or previously repaired holes in this test section. Repairing process involved two steps: The first step was to fill the micro or milli scale map-cracks developed in the old ILPC with MMA polymer by a vacuuming-impregnation method; the second was to coat the entire surface of the MMA-impregnated old ILPC dike with the water compatible, non-flammable, and anti–UV epoxy. Table 14 gives the formulations represented as the total weight percents for these material systems.

The vacuuming-impregnation operation in the first step was conducted in the following sequences: 1) A strip of extremely sticky double-sided tape was applied three inches inside the perimeter of the panel (Figure 32); 2) two one inch mesh fabric nets were evenly laid out within this tape border; 3) three inverted troughs (six-in. diam. x approximately 5-ft.long) with closed ends and a two inch pipe nipple coming out the top were evenly spaced on the panel (Figure 33); 4) the ends of five clear plastic tubes (½ in. inside diameter) then were placed within the area to be impregnated at various locations and the other ends of the tubes were run to the top of the dike; 5) the latter were sealed to prevent vacuum leakage; 6) the tubes were crossed with sticky tape to hold them in place and another layer of tape was applied over the tube; 7) a six mil sheet of reinforced polyethylene was placed over the slab and carefully sealed to the sticky perimeter tape (Figure 34); 8) gaps for the three, two inch pipe nipples coming out of the top of the troughs were cut through the polyethylene sheet, and then this sheet was sealed around them; 9) two inch diameter hoses were connected from these nipples to a valved manifold connected to the vacuum pump at the top of the dike (Figure 35); 10) the vacuum pump was turned on and the valves opened; the polyethylene sheet immediately sucked in tight to the panel (Figure 36); 11) the MMA monomer was mixed with the BPO catalyst (Figure 37); 12) after vacuuming for 40 minutes, the ends of the five sealed tubes that were previously run to the top of the dike were opened and inserted into a five gallon can of MMA (Figure 38); 13) the MMA monomer was immediately drawn out from the container and was observed to rapidly spread out under the polyethylene sheet covering about 45% of the surface (Figures 39 and 40), while the vacuum continued to run; 14) during this 12 minute impregnation, ~ 14 gallons of MMA were consumed to fill the cracks in the panels' surfaces; 15) the polyethylene sheet was peeled off from the panel (Figure 41); 16) of the total area of panel, about 95 % was wetted by MMA (Figure 42); and finally, 17) additional MMA was poured on the remaining ~ 5 % non-wetted areas and rolled into the surface until it ran off (Figure 43).

The following day, ~ 12 hours after the impregnation of MMA monomer, we observed as expected that the impregnated MMA was completely cured. The repairing operation now shifted to overlying the water-compatible, non-flammable and anti–UV epoxy coating on the MMA-impregnated dike. In preparing the FX-489 Epoxy topcoat

consisting of two parts, first, appropriate amounts of the three additives, the fire retardant, anti-oxidant and silane coupling reagent, were added to three gallons of epoxy (designated as part A), and this mixture was stirred with a motorized mixer (Figure 44); second, the one gallon can of part B was added to it, followed by mixing. The prepared epoxy resin was poured on the panel from the top downward, spread with a squeegee and then rolled with a paint roller into the surface (Figure 45). All 4.5 gallons of the epoxy was used for the first coating layer. The epoxy coating was cured within four hours. Afterward, a second epoxy coating totaling there gallons was applied in a similar fashion to the first layer's surface (Figure 46). A graded sand mixture was broadcast over the top layer before it gelled to provide a skid resistant surface. Figure 47 compares the appearance of the repaired and non-repaired ILPC dikes' surfaces.

4.6. Post-field Test Analyses

Nearly two weeks after being repaired, a core sample, ~ 2 in. diam. by ~ 3.5 in. long, was taken from a location of ~ 2 ft. away from the bottom edge of the repaired 8-ft.-wide x 30-ft.-length ILPC-overlay slop panel using a drilling bit (Figure 48). The core sample (Figure 49) was brought to BNL to conduct the post-demonstration analyses, to provide us with pivotal information on whether the vacuuming-impregnation repairing technology and subsequent deposition of a top coating layer has the potential and reliability for restoring a 16-year-old damaged ILPC overlay. As revealed by the cross-sectional area, the corrected core sample was composed of four layers; the epoxy top coating, MMA-impregnated old ILPC, MMA layer linked between impregnated ILPC and underlying concrete, and the concrete. For comparison purpose, we took a reference core sample from the non-repaired ILPC overlay (Figure 50). The post-demonstration analyses focused on assessing the reconstitution and restoration of damaged ILPC overlay by this repairing technology. They involved classifying the failure modes by the tensile splitting test and identifying the chemical states by FT-IR. Figure 51 shows photographs of the failure modes for the repaired and non-repaired core samples after the tensile splitting test. In the repaired core sample (Figure 51, left), most of the splitting breakage took placed in the underlying concrete layer, except for a remnant of ~ ½ in. thick concrete layer attached to the ILPC. No conspicuous feature of destruction was

observed from the repaired ILPC, except for one single centerline crack in the coating layer's surface. This failure mode can be taken as evidence that the copious voids and cracks existing in the old ILPC were filled by MMA polymer, thereby leading to its reconstitution; the filled MMA polymer structurally bonded the cracks and disrepair or broken pieces together again, and also established links between the delaminated ILPC overlay and underlying concrete. Furthermore, it is possible to assume that some MMA might permeate into the underlying concrete to reinforce it, explaining why a layer of undamaged ~ ½ in. thick concrete remained attached to the ILPC after the tensile test. In fact, a strong odor of non-cured MMA emanated from the broken concrete. In contrast, the non-repaired core sample was broken easily throughout it (Figure 51, right).

Figure 52 shows the FT-IR spectra for the samples taken from the non-impregnated (top) and MMA-impregnated (bottom) ILPC layers. The FT-IR spectrum of former included absorption bands at 3524.9, 3461.5, 2927.2, 2860.5, 1648.7, 1507.7, 1454.8, 1237.4, 1178.6, 1020.0, 802.6, and 661.5 cm^{-1}. The bands at 3524.9 and 3461.5 cm^{-1} were attributed to the O-H stretching vibration in moisture. Correspondingly, the band at 1648.7 cm^{-1} belonged to the H-O-H bending vibration in moisture. The three bands at 2927.2, 2860.5, and 1454.8 cm^{-1} were assignable to the stretching mode of $-CH_2-$ within the polyester binder. Considerable attention is concentrated on the bands at 1507.7 cm^{-1} originating from the carboxylate anion group, $-COO^-$. No ester group (-CO-O-)-related band at ~ 1730 cm^{-1} was found in this spectrum, strongly suggesting that the ester groups in the original polyester binder were transformed into the carboxylate anion groups during a long period of 16 years. Thus, it is possible to rationalize that the ester groups in polyester polymer structure underwent the UV-promoted saponification and were converted into the carboxylate groups, implying that the polyester-based binder in the ILPC was degraded. This degradation might cause some shrinkage of ILPC that would be reflected in the generation of numerous cracks. All remaining bands of the spectrum were associated with the aluminum silicate microsphere fillers used as the thermal insulator of ILPC. Compared with that of the non-impregnated ILPC layer, the spectrum of the impregnated layer was characterized by the incorporation of an additional band at 1731 cm^{-1} (see arrow), attributed to the ester groups ($-CO-O-CH_3$) in MMA,

clearly verifying that MMA had permeated into the damaged ILPC during the vacuuming-impregnation process.

These results from the post-demonstration analyses strongly suggested that this repairing technology has a high potential for restoring and rehabilitating 16-year-old ILPC.

5. Material Costs

Based upon the above information, we made a rough cost estimate of two material systems: One system was that we already used for restoring the damaged 8-ft. wide x 30-ft. long ILPC panel; the other would be used for patching small potholes (1-ft. x 1-ft. square and 1-in. deep). For the first system, the cost analysis was based upon the formulation of repairing material systems (Table 14), the cost of raw materials (Table 15), and the total amount of materials used in this 8-ft. wide x 30-ft. long ILPC panel. As estimated, the total cost of material was $ ~ 920 (Table 16), of which ~ 65 % was taken by MMA used in the vacuuming-impregnation operation. For the pothole, material that can be put in place with a hand tool would patch it, comparable treating it as a local failure of ILPC panel. The surfaces of the placed material then are troweled to attain a smooth surface texture. Tables 17 and 18 give the formulation of this material and the cost of raw materials, respectively; we calculated that this material would cost $ ~ 17/ft^2 (Table 19).

6. Conclusions

A little more than sixteen years after the surfaces of a cement concrete-based floor and sloped walls of a dike at a liquefied natural gas (LNG) facility in Greenpoint, Brooklyn, NY, were covered with ~ one inch thick insulating lightweight polymer concrete (ILPC) consisting of polyester as the matrix and lightweight multi cellular glass beads as the thermally insulating aggregates, the polyester binder underwent the ultraviolet (UV) radiation-catalyzed degradation, causing it to became susceptible to the saponification during its long-term exposure in an atmospheric environment. Although the ILPC retained its insulating property, the combination of long-term UV exposure and hydrolysis damage led to the shrinkage of the overlay structure, promoting the

delamination of the ILPC from the underlying concrete and generating copious fissures in its layer. There were primarily three types of destruction to be repaired: First, potholes created by the spalling of the ILPC; second, uplifting of the ILPC caused by its delamination from the underlying concrete; and, third, map cracks that developed in the ILPC's surfaces. All these types of destruction were observed on the sloped sidewall panels; the principal destructive mode of the floor overlay was the last type.

Based upon the failure assessments of the overlays described above, three commercial repairing technologies were evaluated in this study: One was the premix-placement method of the material system consisting of a high viscose organic resin as the binder and the insulating lightweight filler for patching the potholes; the second was the vacuum-impregnation sealing method using a very low viscose, good wicking monomer containing an appropriate amount of catalyst for restoring the structural and surface integrity of the dormant cracks and delaminated areas and for repairing the map cracking developed in the superficial and subsurface areas of floor; and, the third was the coating-finishing method for the repaired overlay surfaces as well as the patched surfaces. The major contribution of the second method was to rebind structurally the cracks and hold the disrepaired or broken pieces together, and also to rejoin the spaces between the delaminated overlay and underlying concrete. Therefore, this program was intended to develop, process, and characterize the repair material systems for the premix-placement, vacuum-impregnation, and top coating finishing methods.

In the premix-placement method, the polymer concrete (PC) systems containing the pressure-resistant hollow micro-sized spheres as the insulating aggregate were required to meet eight essential material criteria for the insulating lightweight pothole-patching materials. Those criteria are addressed as follows; 1) moderate plasticity and an appropriate pot life of the ILPC slurry, 2) compressive strength of > 1500 psi, 3) density of < 50 Ib/ft^3 (< 0.8 g/cc), 4) flexure strength of > 600 psi, 5) thermal conductivity of < 0.13 Btu/hr-ft-°F, 6) excellent adherence to both the cement concrete and polyester-based old ILPC, 7) non-flammability, and 8) excellent resistance to UV. To meet these criteria, we formulated an epoxy-based PC consisting of 40.3wt% epoxy as binder part A (ChemCo Systems, Inc), 17.3wt% polyamines catalyst as binder part B (ChemCo Systems, Inc.), 31.0wt% aluminum silicate ceramic-shelled microspheres as the

lightweight thermal insulator (PQ Corporation), 8.7wt% ammonium polyphosphate as the flame retardant (Clarian Corp.), 1.8wt% 2,4-di-tetriary-butylphenyl phosphate as the anti-oxidant (Uniroyal Chemcial Corp.) and 0.9wt% aminopropylsilane triol as the silane coupling agent (Gelest Inc.). This formulated PC had a slurry density of 47.50 lb/ft^3 (0.76 g/cc), a compressive strength of 2050 psi, a flexure strength of 2000 psi, a thermal conductivity of 0.041 to 0.043 Btu/hr-ft-°F, at the cryogenic atmospheric temperature of –260°F, and interfacial bond strengths of 71.7 psi and 36.4 psi at the joints between epoxy-based PC, and polyester-based old dry and wet ILPC, respectively, along with 69.2 psi and 51.1 psi bond strengths at the epoxy PC/dry and wet concrete joints, respectively. This material costs \$17.24/ft^2 for repairing a 1-ft. x 1-ft. x 1-in. pothole.

For the vacuum-impregnation sealing method, a methyl methacrylate (MMA) monomer (Fox Industries Inc.) with a low viscosity of ~ 15 cps was used as a wicking material that could permeate through a narrow crack with a length of at least 1 inch to the depth of 0.5 inch. The curing time of MMA depended primary on the content of benzoyl peroxide (BPO) catalyst used to initiate curing (Fox Industries Inc.) at a room temperature. The most effective content of BPO was 2 % by weight of that total amount of MMA; it allowed the MMA to penetrate satisfactorily through the fractures and crack networks, and also had a pot life of around 20 min after mixing the MMA and BPO. In the in-house study using a vacuum-impregnation chamber designed by BNL, a vacuum at a -28 in.Hg, eliminated any air and moisture entrapped in the fractures in ILPC and in the interstices between the ILPC and underlying concrete. Correspondingly, the 2wt% BPO-catalyzed MMA monomer easily permeated through fine cracks below 0.004 in. in width, and also filled the interstices between the ILPC and the underlying cement concrete. The latter activity played a pivotal role in rebonding the delaminated, lifted ILPC to the underlying concrete because the MMA that cured in this interstice offered a strong coupling between the delaminated ILPC and concrete. In fact, when both the old polyester-based ILPC and concrete adherends were dry, the bond strength of the MMA adhering to them was as strong as 42.2 psi. However, if both adherends were wet, strength fell ~ 41 % to 24.9 psi.

The major thrust of the coating-finishing method was to confer advanced properties on the commercial epoxy floor coating (Fox Industries Inc.) by modifying it

with flame retardants, UV-resistant reagents, and silane coupling agents. Among the several flame retardants, the most effective one in making a non-flammable epoxy coating was ammonium polyphosphate known by the trade name “Exolite AP 422” (Clarian Corp.); its most effective amount was 15 % by weight of the total amount of epoxy. Adding this flame reatardant not only suffocated fire in the coating, but also increased compressive and flexure strengths by ~34.5 % and ~39.3 %, respectively. Additionally, it did not impair the adherence of the epoxy to the MMA-repaired polyester-based old ILPC and the patch-repair material surfaces.

Organic polymers significantly absorb the UV radiation present in the solar spectral region reaching the earth’s surface (wavelength, λ, > 300 nm), leading to the incorporation of oxygen into the their structure. Thus, photo degradation damage was one of the important improvements needed for the coating. Results from exposure test to a portable high intensity UV lamp having a wavelength of 366 nm revealed that the antioxidant tris (2,4-di-tetriary-butylphenyl)phosphate (TTBH, Uniroyal Chemical Corp.) displayed a best performance in inhibiting the rate of UV-caused damage of this epoxy coating; the appropriate amount to add was 2 % by weight of the total epoxy content.

The water-compatibleness of the coating was another important factor governing its adherence to wet repaired ILPC and patching material surfaces; making it enable to increase the ability of coating to protect the restored underlying overlays against fire and UV. Therefore, we evaluated the usefulness of aminopropylsilane triol (APST, Gelest Inc.), a silane coupling agent in achieving this goal. When a coating without APST was applied to wet MMA surfaces, the bond strength developed at interfaces between the coating and the wet MMA was only 99 psi. This strength rose by nearly twice once this coating was modified with 1% APST by weight of the total amount of coating. Thus, the APST had high potential as a chemical additive that enhances the water-compatibleness of the epoxy coating.

From the integration of all information on the coating, the following optimized formulation for the epoxy coating can be proposed: 56.5wt% epoxy (FX-489 Part A), 28.2wt% epoxy (FX-489 part B), 12.7wt% ammonium polyphosphate anti-flammable reagent (Exolite AP422), 1.6wt% 2,4-di-tetriary-butylphenyl phosphate anti-UV reagent (Naugard 524), and 1.0wt% aminopropylsilane triol silane coupling agent (SIA 0608).

Two different types of the interfacial bond durability tests were carried out to assess how well the coating adhered to the wet MMA-impregnated ILPC surfaces: One was that the coating surfaces were exposed to liquid nitrogen (LN) at the cryogenic temperature of –209.9°C (-345.8°F) assuming that liquefied natural gas (LNG) at -160°C (-260°F) was spilled over the coated ILPC overlay surfaces; the other referred to the freeze-thaw cycling as per ASTM C666. For the former test, the results revealed that neither delaminations nor blisters were observed from the coating's surfaces after 24 hours exposure, underscoring that although the surfaces of MMA-impregnated ILPC overlay were wet, the BNL-formulated epoxy coating strongly adhered to the wet MMA. More importantly, the coating/MMA-impregnated ILPC/concrete joint structure remained intact. For the latter test, specimens subjected to a series of 6 freeze-thaw cycles per 24 hours based upon a one cycling temperature between 0 and 50°F showed no changes in appearance after 200 cycles; there was no delamination of the top coating layer. Thus, bond durability at the coating/MMA-impregnated ILPC/concrete joints was outstanding in the 200 freeze-thawing cycles.

Since the total areas requiring patch repairing were negligible, our focus in small-scale field test concentrated on evaluating the technical feasibility of the vacuuming-MMA impregnation-epoxy coating method for repairing dormant- and map-cracked old ILPC overlay. On September 21-22, 2004, a field demonstration was performed at the KeySpan liquefied natural gas (LNG) facility in Greenpoint, Brooklyn NY, under the contract with the Balvac Inc. A sloped sidewall panel, 8-ft. in wide x 30-ft. in length was selected for this field test. The repairing process was carried out in the following sequence: 1) adhesion of extremely sticky double-sided tape to the perimeter of the test panel; 2) placement of two one inch mesh fabric nets within this tape border; 3) deployment of three inverted closed end troughs (six-in. diam. x approximately 5-ft.long) including a two inch vacuuming pipe nipple over the mesh fabric nets; 4) placement of five ½ in. diam. clear plastic tubes to transport the catalyzed MMA monomer; 5) coverage of the test panels' surfaces by a six mil thick polyethylene sheet sealed to the sticky perimeter tape; 6) connecting the two inch diameter vacuuming hoses and the two inch pipe nipples coming out of the top of the troughs; 7) applying a vacuum for 40 minutes; 8) impregnation of BPO-catalyzed MMA monomer in the fissured ILPC layers

while continuing vacuuming; 9) removal of the polyethylene sheet from the test panel after ~ 12 minutes impregnation; 10) treatment of some non-wetted panel areas with additional MMA; 11) cure of impregnated MMA within ~ 12 hours after completing this operation; 12) coating of MMA-impregnated ILPC panel surfaces with the water-compatible, non-flammable, and anti–UV epoxy material; 13) cure of coating within four hours after deposition on the panel surfaces; 14) application of second epoxy coating to the first coating's surface; and, 15) broadcasting a graded sand mixture over the top layer to create a skid resistant surface.

Nearly two weeks after being repaired, a core sample, ~ 2 in. diam. by ~ 3.5 in. long, was taken from a location of ~ 2 ft. away from the bottom edge of the repaired 8-ft.-wide x 30-ft.-length ILPC-overlay sloped panel using a drilling bit. The core sample was brought to BNL for post-demonstration analyses to provide us with pivotal information on whether the vacuuming-impregnation repairing technology followed by the deposition of top coating layer has the potential and reliability for restoring a 16-year-old damaged ILPC overlay. These analyses focused on assessing the reconstitution and restoration of damaged ILPC overlay. They involved classifying the failure modes by the tensile splitting test and identifying the chemical states by FT-IR. The result strongly demonstrated that the copious voids and cracks existing in the old ILPC were filled by MMA polymer, leading to its reconstitution because the MMA polymer structurally rebonded the cracks and broken pieces, and also established links between the delaminated ILPC overlay and underlying concrete. Accordingly, this repairing technology had a high potential for restoring and rehabilitating the 16-year-old ILPC.

Based upon our use of ~ 14 gallons MMA for the impregnating operation along with ~ 7.5 gallons epoxy for the coating operation of two layers in this field demonstration, the estimated total cost of materials was $ ~ 920 for restoring the damaged 8-ft. wide x 30-ft. long ILPC; ~ 65 % of this amount was due to the MMA used in the vacuuming-impregnation operation.

Appendix 1: Program Expenditure

The total completion cost of this program for the period of February 2003 through January 2005 was $180,000. A month-by-month graphical representation of this program's expenditure is presented in Figure 53.

Table 1. Properties of epoxy and polyurea binders

Binder	Viscosity at 25°C, cp	Gel time at 25°C, min	Tensile strength, psi	Elongation at break, %
Epoxy	285	25	2200	60
Polyurea	700	25	1000	225

Table 2. Formulation and density of ceramic microsphere-filled polyurea lightweight polymer concretes

Sample No.	Polyurea (part A), wt%	Polyurea (part B), wt%	Ceramic microsphere, wt%	Density of cured sample, lb/ft^3 (g/cc)
PUR-1	47	43	10	63.12(1.01)
PUR-2	42	38	20	58.13(0.93)
PUR-3	39	36	25	55.63(0.89)
PUR-4	37	33	30	51.88(0.83)
PUR-5	34	31	35	50.00(0.80)
PUR-5	26	25	49	46.05(0.74)
PUR-6	23	22	55	46.88(0.75)

Table 3. Formulation and density of ceramic microsphere-filled epoxy lightweight polymer concretes

Sample No.	Epoxy (part A), wt%	Epoxy (part B), wt%	Ceramic microsphere, wt%	Density of cured sample, lb/ft^3 (g/cc)
EP-1	63	27	10	65.27(1.04)
EP-1	56	24	20	60.63(0.97)
EP-2	53	22	25	57.50(0.92)
EP-3	49	21	30	53.13(0.85)
EP-4	46	19	35	51.88(0.83)
EP-5	36	15	49	47.50(0.76)
EP-6	31	14	55	41.88(0.67)

Table 4. Bond strength at the joint between the PC patching materials and the damaged old ILPC or cement concrete adherends for specimens aged for 3 days.

PC patching material	Surface of damaged old ILPC	Surface of cement concrete	Bond strength, psi	Adhesion failure mode
Epoxy	Dry		71.7	Cohesive failure in cement concrete
Epoxy	Wet		36.4	Adhesive failure at interface
Epoxy		Dry	69.2	Cohesive failure in cement concrete
Epoxy		Wet	51.1	Mix mode of cohesive and adhesive failures
Polyurea	Dry		36.7	Cohesive failure in polyurea
Polyurea	Wet		13.5	Adhesive failure at interface
Polyurea		Dry	54.0	Cohesive failure in polyurea
		Wet	10.1	Adhesive failure at interface

Table 5. Gel time of MMA containing 1.5, 2.0, 3.0, and 5.0wt% BPO initiator at room temperature.

BPO content by weight of MMA, %	Gel time, min
1.5	28
2.0	17
3.0	11
5.0	7

Table 6. Visual observations of the defective topping ILPC disk/cement concrete joints after impregnation of MMA under vacuum and normal conditions.

Vacuum	Range of crack's width, in.	Penetration of MMA	Filling activity of MMA in the interstices between ILPC disk and concrete
Yes	0.003-0.007	Excellent	Fully filled (Figure 15)
Yes	0.009-0.013	Excellent	Fully filled
Yes	0.021-0.025	Excellent	Fully filled
No	0.003-0.007	No penetration	No filling
No	0.009-0.023	Some penetration	No filling
No	0.021-0.0025	Good	Partially filled

Table 7. Bond strength at the joint between the MMA repairing materials, and the old ILPC and cement concrete adherends.

Surface of damaged old PC	Surface of cement concrete	Bond strength, psi	Adhesion failure mode
Dry	Dry	44.2	Mix mode of cohesive and adhesive failures in concrete
Wet	Dry	39.8	Mix mode of cohesive and adhesive failures in concrete
Dry	Wet	22.8	Adhesive failure at interfaces between MMA and concrete
Wet	Wet	24.9	Adhesive failure at interfaces between MMA and concrete

Table 8. Flammability of flame retardant-modified epoxy coatings.

Flame retardants, wt%		Flammability as per ASTM D635*
Exolite AP422	Exolite AP750	
0	0	Burning, rate of burning 2.8 in./min.
1	-	Burning, rate of burning 2.5 in./min.
2	-	Burning, rate of burning 1.8 in./min.
5	-	Burning, rate of burning 1.5 in./min.
10	-	Self extinguishing after ~ 100 sec.
15	-	No burning.
-	1	Burning, rate of burning 2.1 in./min.
-	2	Burning, rate of burning 1.8 in./min.
-	5	Burning, rate of burning 1.6 in./min.
-	10	Self extinguishing after ~ 110 sec.
-	15	Self extinguishing after ~ 69 sec.

* Average of three samples.

Table 9. Change in compressive and flexure strengths of the epoxy specimens as a function of Exolite content.

Exolite, wt%	Compressive strength, psi	Flexure strength, psi
0	4865	1073
5	5340	1205
10	6053	1338
15	6543	1495

Table 10. Bond strength at the joint between the epoxy and the MMA

Exolite, wt%	Surface of MMA	Bond strength, psi
0	Dry	280
0	Wet	99
15	Dry	282
15	Wet	101

Table 11. Comparison between the bond strengths of APTS- and APST-modified epoxy coatings adhering to wet MMA's surface.

Surface's condition of MMA	APTS content, wt%	APST content, wt%	Bond strength, psi	Failure locus
Dry	0	0	290	Mix mode of cohesive failure in epoxy and adhesive failure at interface.
Wet	0	0	99	Adhesive failure at interfaces.
Wet	0.5	0	108	Adhesive failure at interfaces.
Wet	1.0	0	119	Adhesive failure at interfaces.
Wet	3.0	0	121	Adhesive failure at interfaces.
Wet	0	0.5	145	Adhesive failure at interfaces.
Wet	0	1.0	179	Mix mode of cohesive failure in epoxy and adhesive failure at interface.

Table 12. Testing samples made under the four different conditions.

Sample, I.D.	First layer	Second layer	Third layer	Top layer
1	Dry concrete	Penetrated MMA	Dry MMA-impregnated PC	Epoxy coating
2	Wet concrete	Penetrated MMA	Dry MMA-impregnated PC	Epoxy coating
3	Dry concrete	Penetrated MMA	Wet MMA-impregnated PC	Epoxy coating
4	Wet concrete	Penetrated MMA	Wet MMA-impregnated PC	Epoxy coating

Table 13. Formulations of concrete, impregnating and coating materials

Material	Formulation
Concrete	41.3wt% type I portland cement, 20.7wt% silica coarse aggregate, 20.7wt% silica sand, and 17.3wt% water.
Impregnation	98 wt% MMA monomer and 2 wt% BPO catalyst
Coating	84.7wt % epoxy, 12.7wt% anti-flammable reagent, 1.6wt% anti-oxidant reagent, and 1.0wt% silane coupling agent.

Table 14. Formulations of two material systems used in this field demonstration

System	Category	Trade name	Chemistry	Wt%
A	Crack-Repairing	MMA- 821	Methyl methacrylate (MMA)	98
A	Crack-Repairing	FX-821 initiator	Benzoyl peroxide (BPO)	2
B	Coating	FX-489 Epoxy part A	Epoxy resin	56.5
B	Coating	FX-489 Epoxy part B	Epoxy resin	28.2
B	Additive	Exolite AP422 Flame retardant	Ammonium polyphosphate	12.7
B	Additive	Anti-oxidant Naugard 524	2,4-di-tetriary-butylphenyl phosphate	1.6
B	Additive	Silane coupling agent, SIA 0608	Aminopropylsilane triol	1.0

Table 15. Suppliers and cost of raw materials

Material	Supplier	Cost
Methyl methacrylate, MMA- 821 and BPO initiator	Fox Industries Inc. 3100 Falls Cliff Road, Baltimore, MA 21211 Tel; 410-243-8856	$42.5/gal.
Epoxy coating, FX-489 including part A and B	Fox Industries Inc. 3100 Falls Cliff Road, Baltimore, MA 21211 Tel; 410-243-8856	$44.7/gal.
Flame retardant, Exolite AP422	Clarian Corp. 4000 Monroe Road, Charlotte, NC 28205 Tel; 704-331-7000	$2.40/lb
Anti-oxidant, Naugard 524	Uniroyal Chemcial Corp. Middlebury, CT 06749 Tel; 877-948-2668	$5.47/lb
Silane coupling agent, SIA 0608	Gelest Inc. 11 East Street Road, Morrisville, PA 19067 Tel; 215-547-1015	$27.0/lb

Table 16. Total cost of materials used for repairing 8-ft. wide x 30-ft. long ILPC panel

Two-step repairing operation	Total amount of repairing materials used in 8-ft. wide x 30-ft. long panel	Material	Fraction of used materials	Cost
Vacuum-impregnation	~ 14 gallons	Methyl methacrylate, MMA- 821 and BPO initiator	~ 14 gallons	~ 14 gals. x $42.5/gal. = $ ~595
			Subtotal	**$ ~ 595/panel**
Top coating (two layers)	~ 7.5 gallons	Epoxy coating, FX-489 including part A and B	~ 6.3 gallons	~ 6.3 gals. x $44.7/gal. = $ ~ 281.7
		Flame retardant, Exolite AP422	~ 8 lb	~ 8 lb x $2.40/lb = $ ~ 19.2
		Anti-oxidant, Naugard 524	~ 1.1 lb	~ 1.1 lb x $5.47/lb = $ ~ 6.0
		Silane coupling agent, SIA 0608	~ 0.67 lb	~ 0.67 lb x $27.0/lb = $ ~ 18.1
			Subtotal	**$ ~ 325/panel**
			Total	**$ ~920/panel**

Table 17. Formulation of epoxy-based pothole repairing material

Trade name	Chemistry	Wt%
CCS Binder Part A	Epoxy resin	40.3
CCS Binder Part B (catalyst)	Polyamines	17.3
Extendospheres SG lightweight filler	Aluminum silicate ceramic-shelled microsphere	31.0
Exolite AP422 Flame retardant	Ammonium polyphosphate	8.7
Anti-oxidant, Naugard 524	2,4-di-tetriary-butylphenyl phosphate	1.8
Silane coupling agent, SIA 0608	Aminopropylsilane triol	0.9

Table 18. Suppliers and cost of raw materials

Material	Supplier	Cost
CCS Binder Part A and B	ChemCo Systems, Inc., 2800 Bay Road, Redwood City, CA 94063 Tel: 650-261-3790	$5.78/lb
Extendospheres SG lightweight filler	PQ Corporation, P.O. Box 840, Valley Forge, PA 19482 Tel: 610-651-4652	$0.41/lb
Flame retardant, Exolite AP422	Clarian Corp. 4000 Monroe Road, Charlotte, NC 28205 Tel: 704-331-7000	$2.40/lb
Anti-oxidant, Naugard 524	Uniroyal Chemcial Corp. Middlebury, CT 06749 Tel: 877-948-2668	$5.47/lb
Silane coupling agent, SIA 0608	Gelest Inc. 11 East Street Road, Morrisville, PA 19067 Tel: 215-547-1015	$27.0/lb

Table 19. Cost of material used for repairing 1-ft. x 1-ft. x 1-in. pothole

Material	Amount of materials used	Cost
CCS Binder Part A and B	2.47 lb	2.47 lb x $5.78/lb = $14.28
Extendospheres SG lightweight filler	1.33 lb	1.33 lb x $0.41/lb = $0.55
Flame retardant, Exolite AP422	0.37 lb	0.37 lb x $2.4.lb = $0.89
Anti-oxidant, Naugard 524	0.08 lb	0.08 lb x $5.47 lb = $0.44
Silane coupling agent, SIA 0608	0.04 lb	0.04 lb x $27.0/lb = $1.08
Total	**4.29 lb**	**$17.24/ft^2**

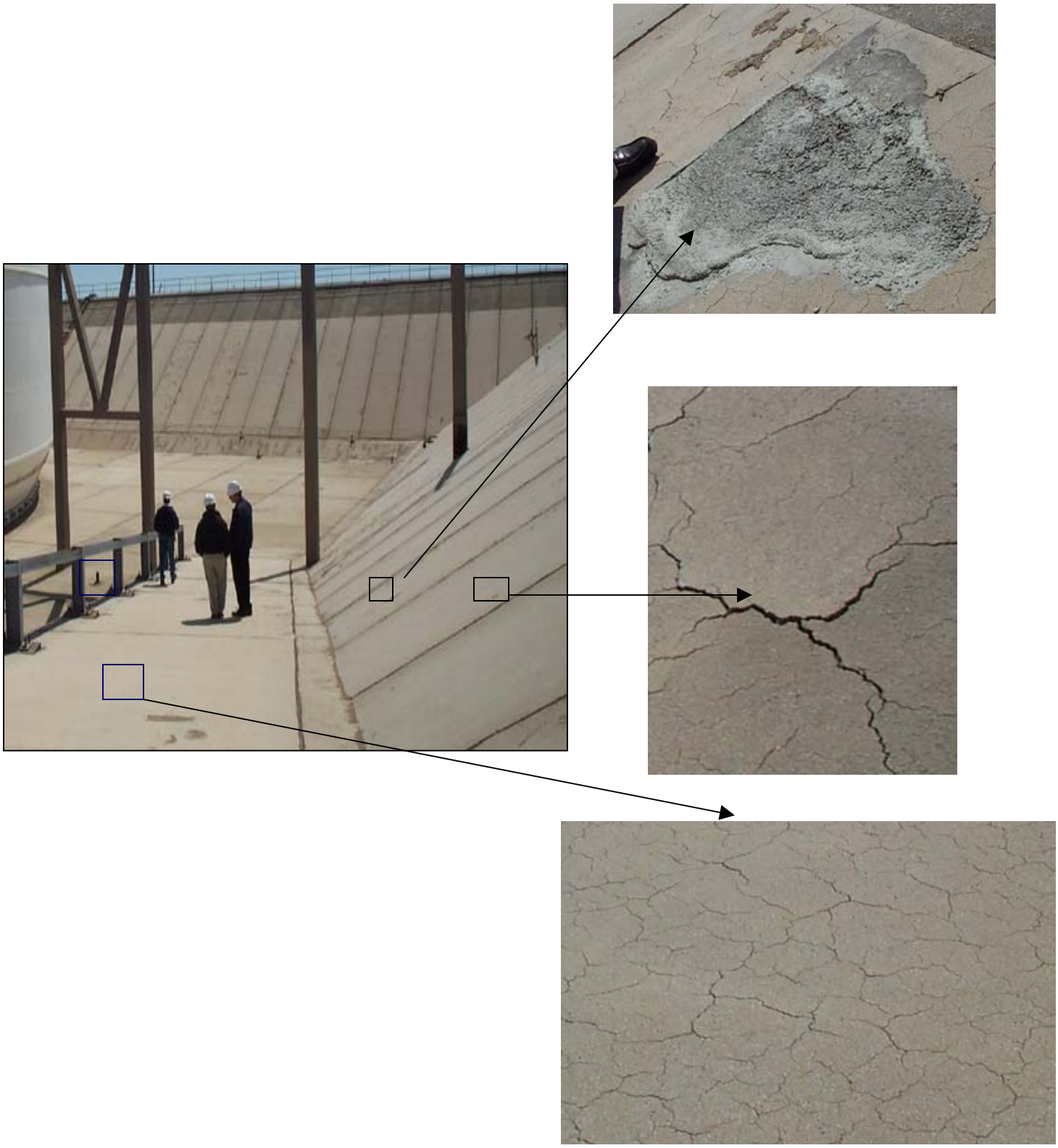

Figure 1. Three types of ILPC's damages, potholes (top), uplift (middle), and map-cracking (bottom).

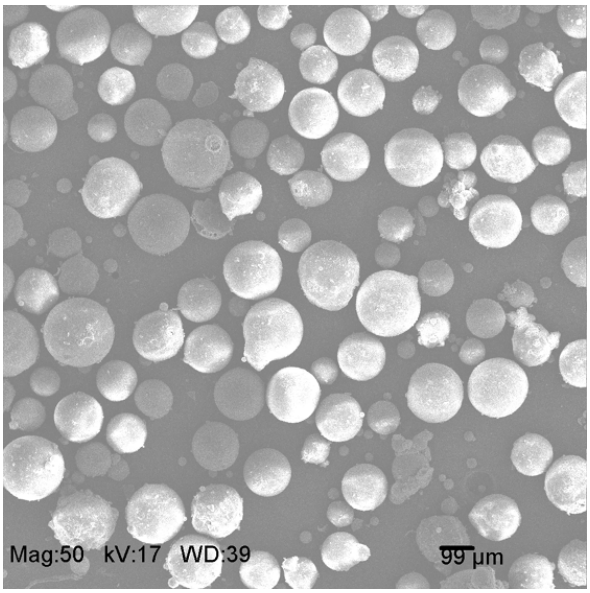

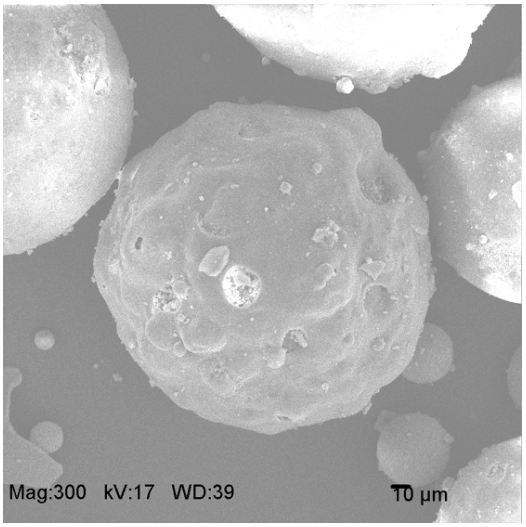

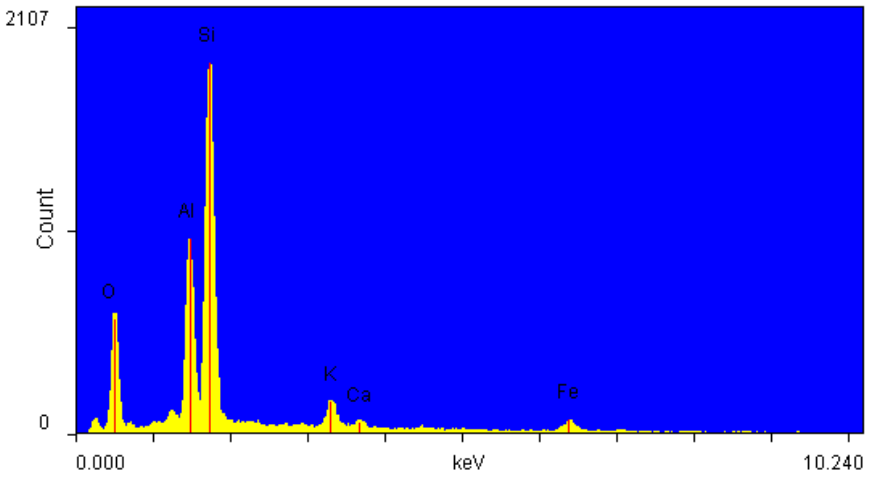

Figure 2. SEM image coupled with EDX elemental analysis for Extendospheres SG

Figure 3. Slump test at 40-degree angle for 55wt% microsphere-filled epoxy and polyurea slurry.

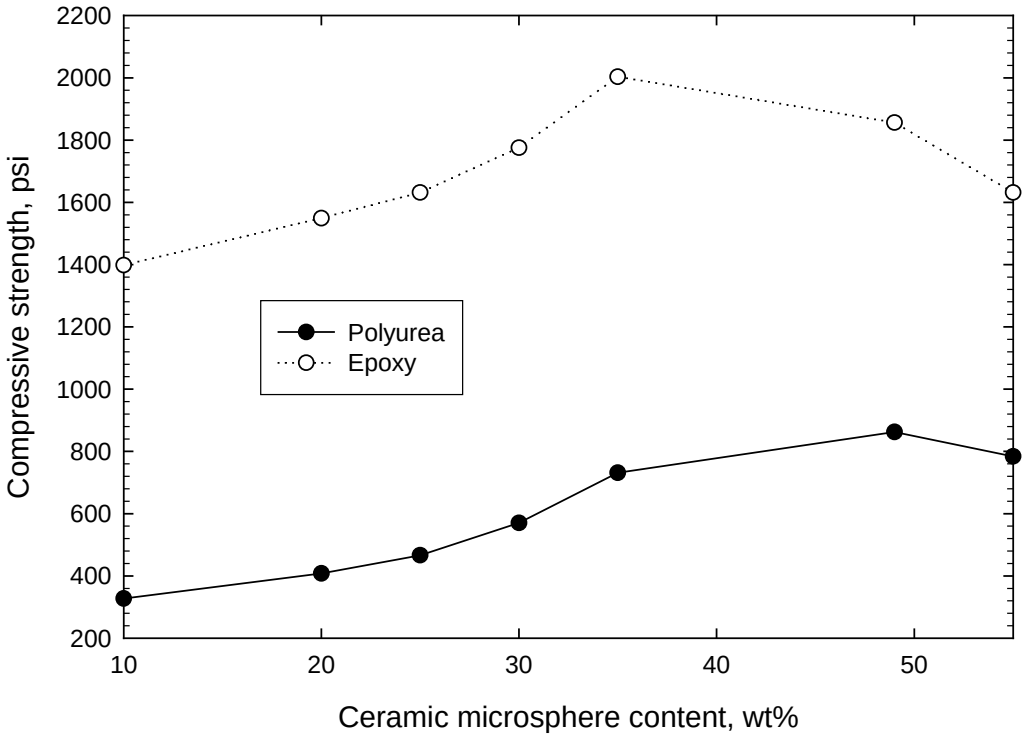

Figure 4. Changes in compressive strength of ceramic microsphere-filled lightweight polymer concrete specimens as a function of microsphere content.

Figure 5. Apparatus for measuring the elastic behavior of polyurea PC specimen.

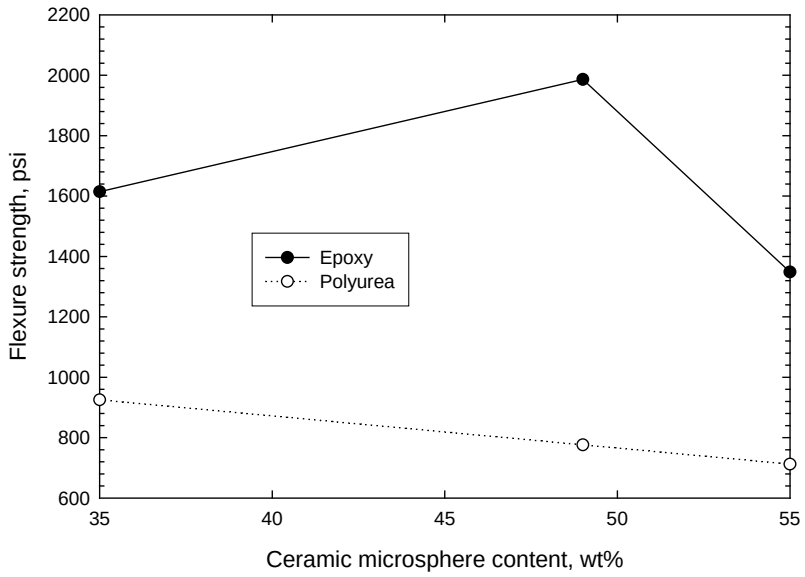

Figure 6. Flexure strength of microsphere-filled lightweight polymer concrete specimens.

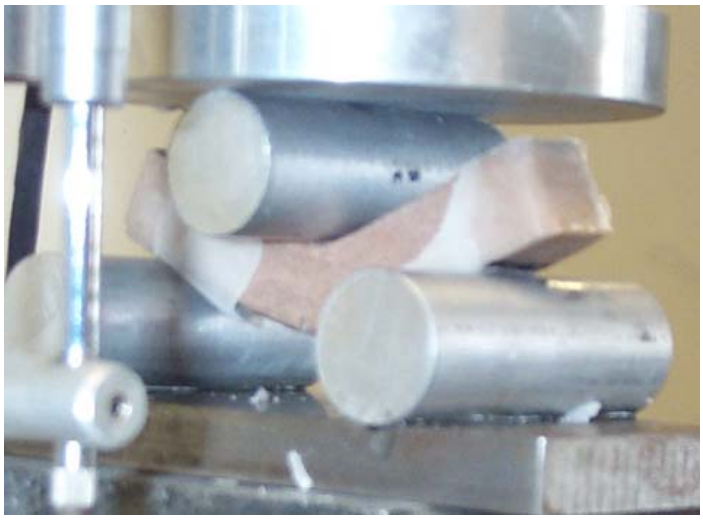

Figure 7. Apparatus for the flexure test for epoxy PC, which displays great ductility.

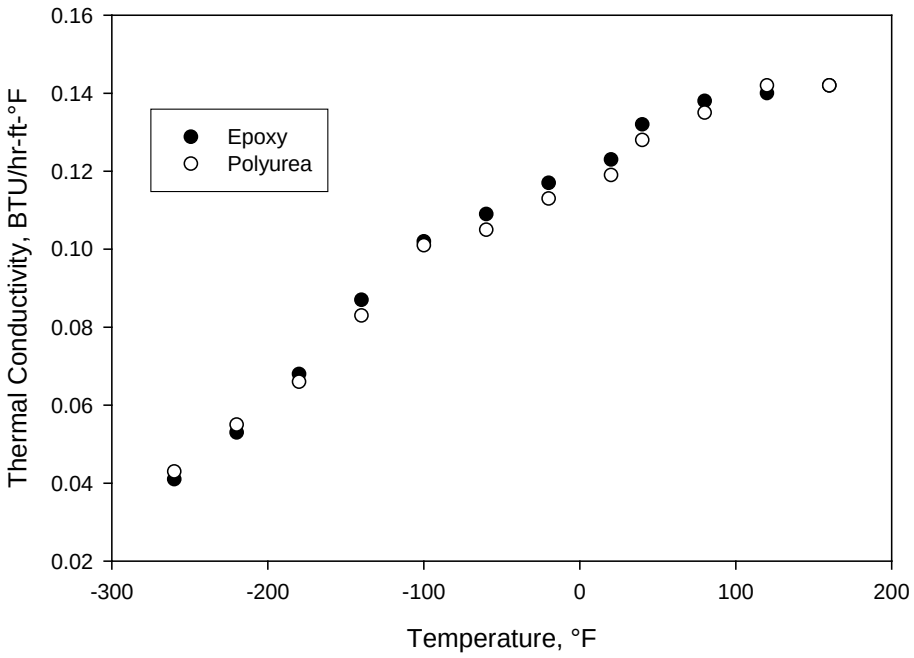

Figure 8. Changes in thermal conductivity of 55wt% microsphere -filled epoxy and polyurea PC specimens as a function of temperature.

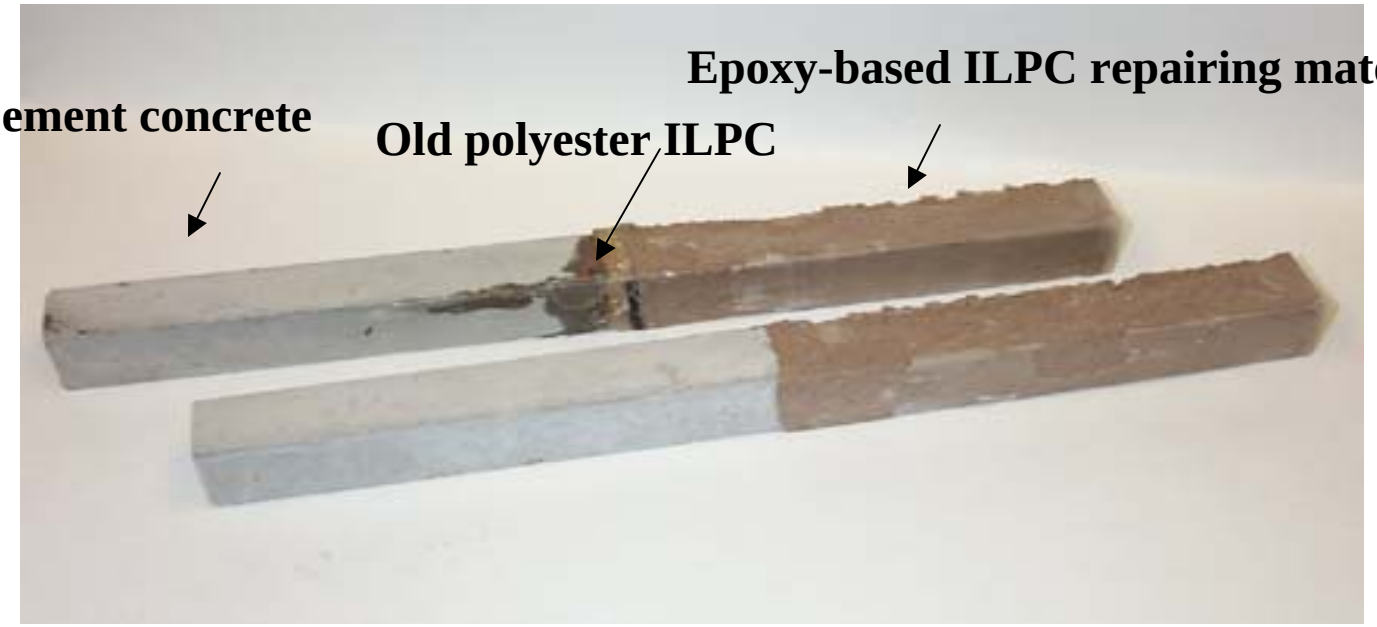

Figure 9. PC patching material/old polyester ILPC/cement concrete joint specimen (top) and PC patching material/cement concrete joint specimen (bottom).

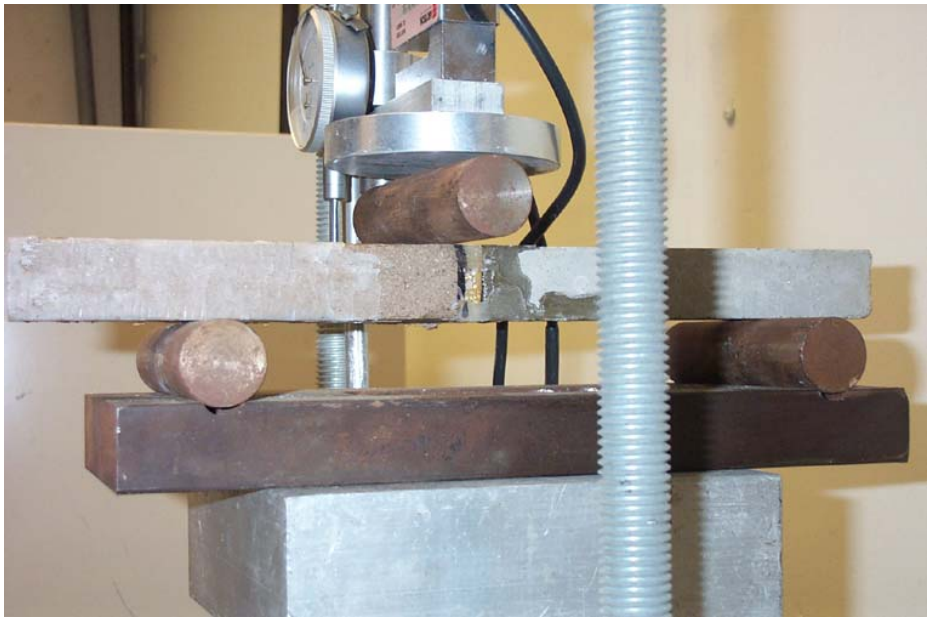

Figure 10. Bond strength test at interfaces between the PC patching material and the old polyester-based ILPC.

Figure 11. Feeler gauges used to fabricate a certain range of crack's width in the ILPC disk.

Figure 12. Feeler gauges embedded in ILPC disk of ~ ½ in. thick (right) and cement concrete made in plastic mold (left).

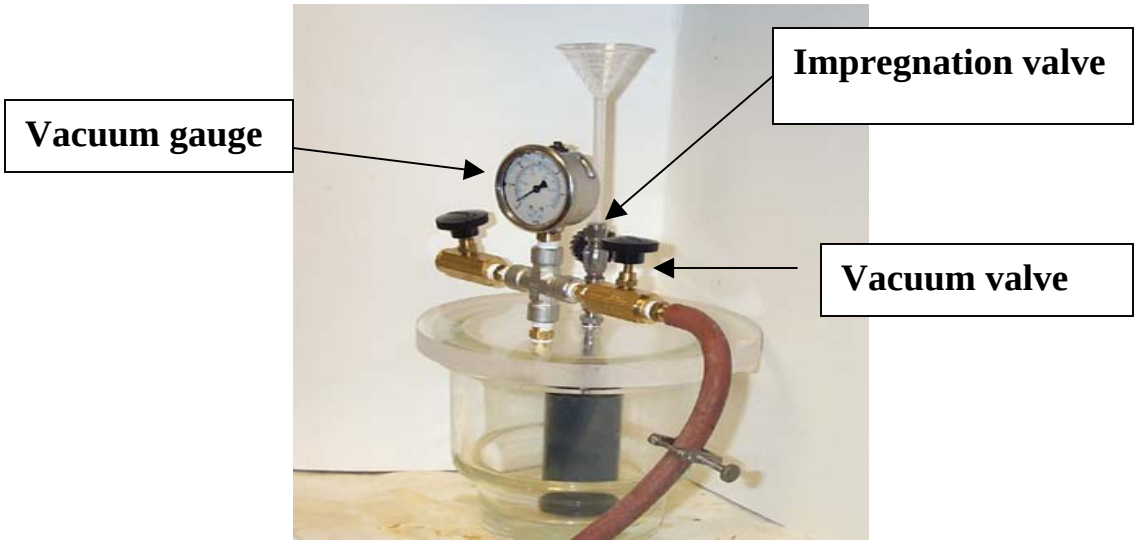

Figure 13. Plastic mold containing topping ILPC disk in conjunction with concrete emplaced in the vacuuming-impregnation chamber.

Figure 14. Injection of catalyzed MMA monomer on to the defective ILPC disk surfaces after10 min. vacuuming.

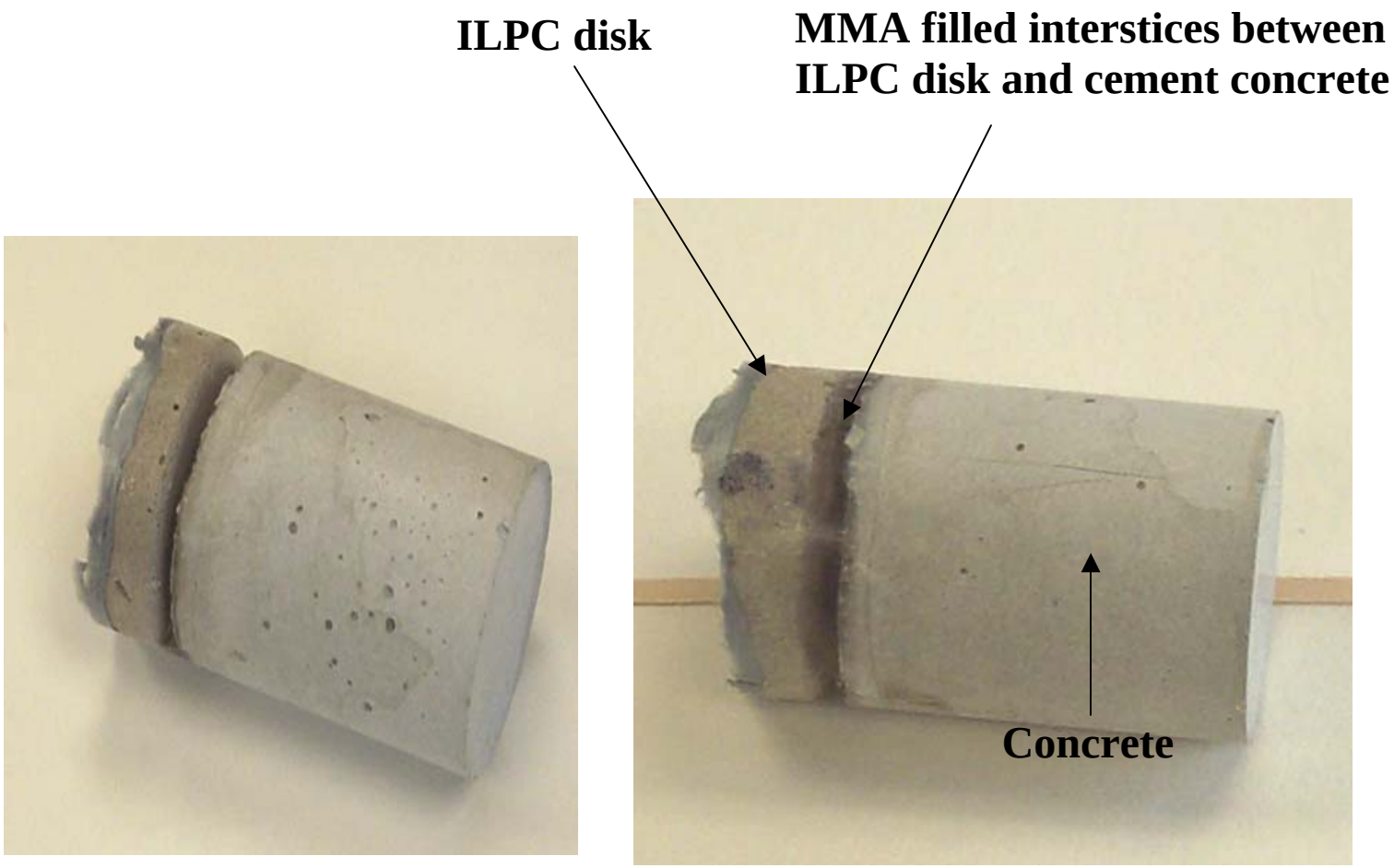

Figure 15. Non-bonded ILPC disk with concrete (left) before impregnation of MMA and the ILPC disk linked to concrete after its impregnation (right).

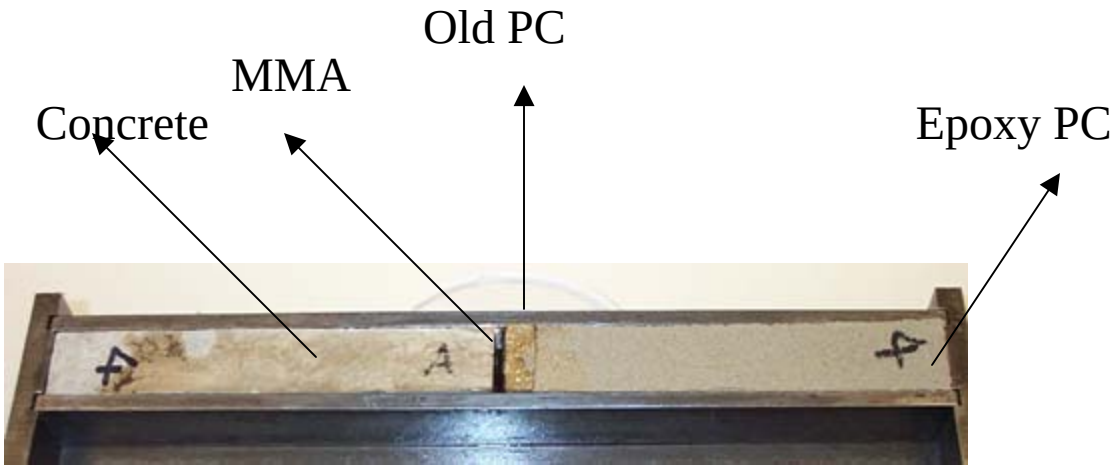

Figure 16. MMA-to-old ILPC and concrete joint specimen prepared in beam mold.

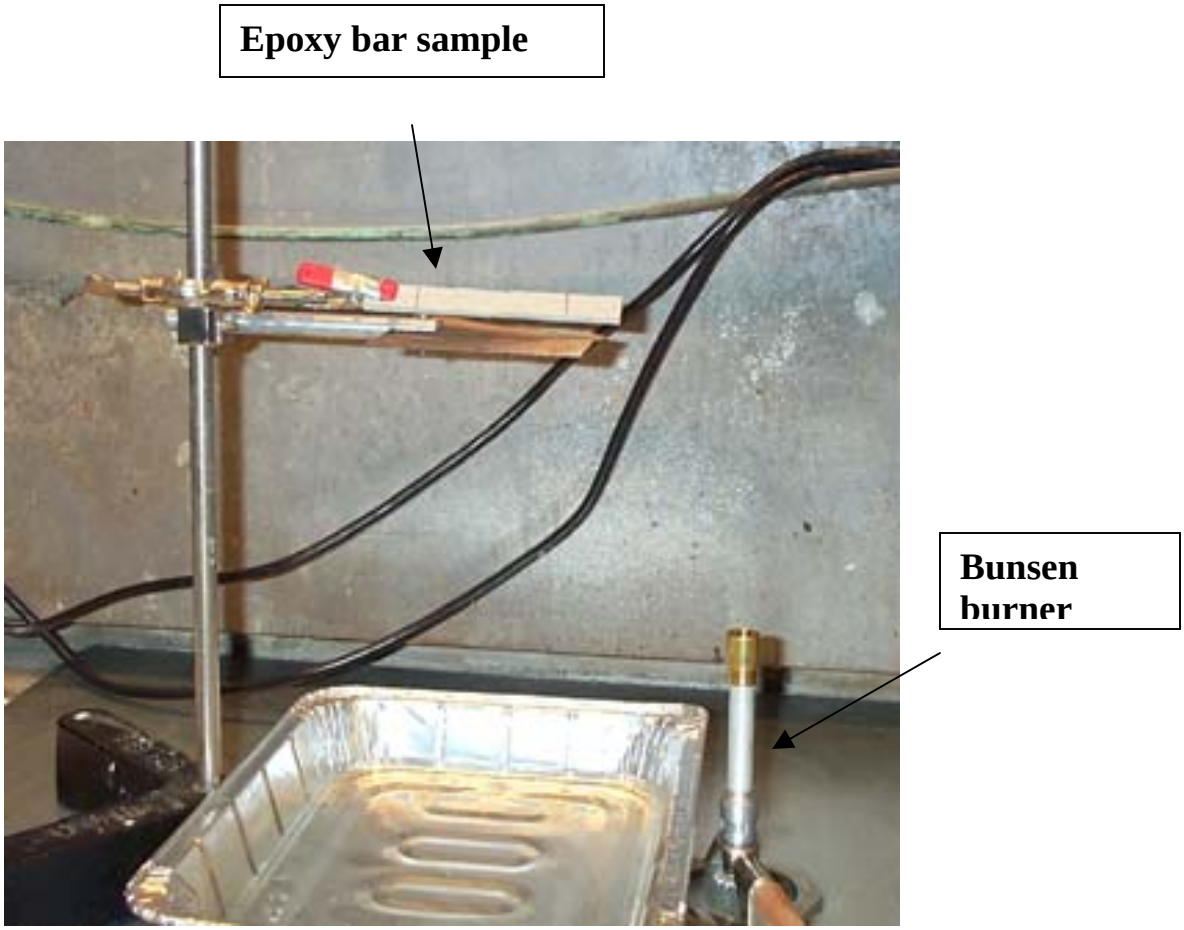

Figure 17. Flammability test in accordance with ASTM D 634.

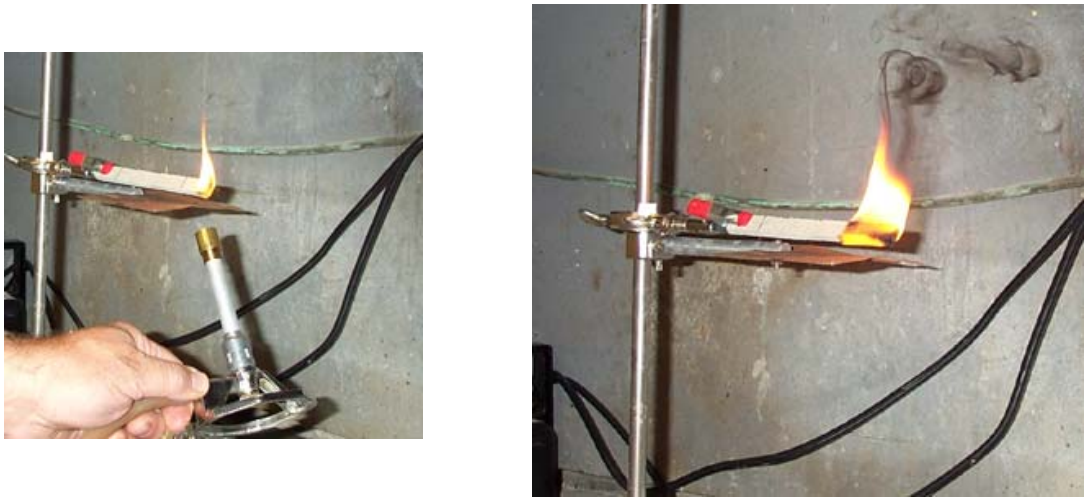

Figure 18. Flammability test for bulk epoxy coating: Ignited fire (left) and burning sample (right).

Figure 19. In a little less that ten seconds after being ignited, the flame extinguished itself, demonstrating the characteristic failure of burning of the material.

Figure 20. UV exposure test for coated aluminum panels.

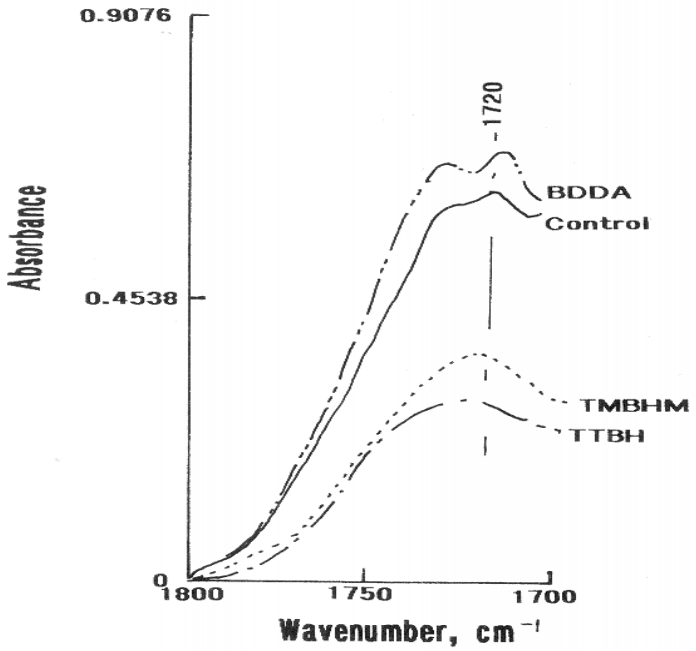

Figure 21. FT-IR absorbance at 1720 cm-1 for 1.0wt% various antioxidant-modified and unmodified epoxy samples after exposure for 6 days to UV radiation.

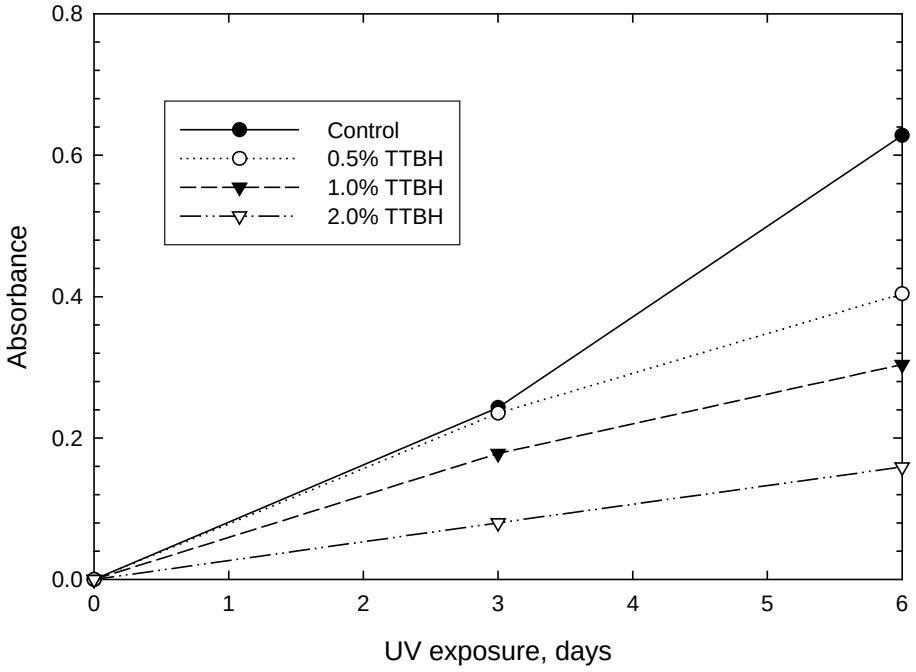

Figure 22. Absorbance at 1720 cm^{-1} for unmodified, and TTBH-modified epoxy samples after exposure for 3 and 6 days to UV radiation.

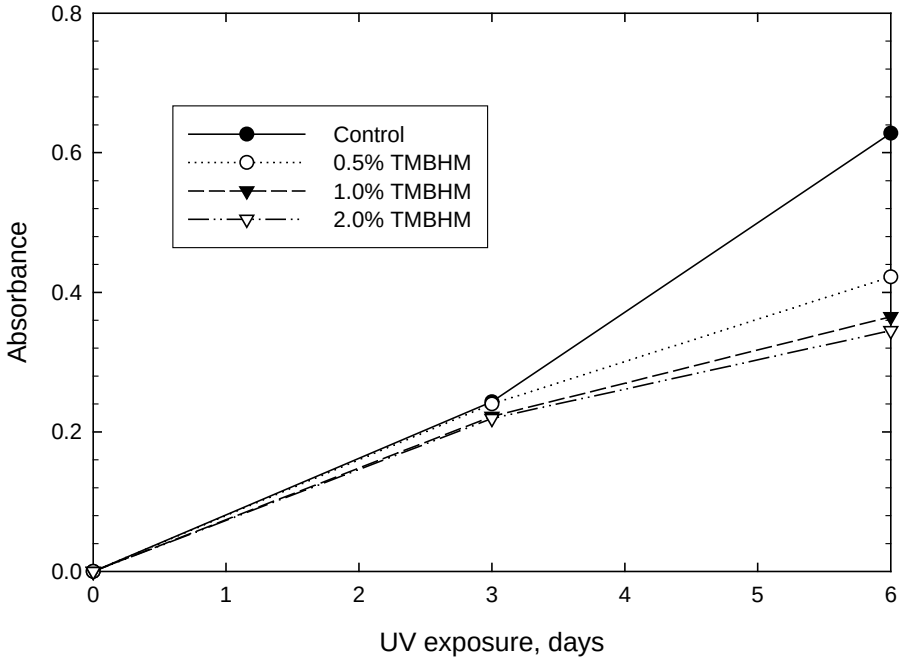

Figure 23. Absorbance at 1720 cm^{-1} for unmodified, and TMBHM-modified epoxy samples after 3 and 6 days exposure to UV.

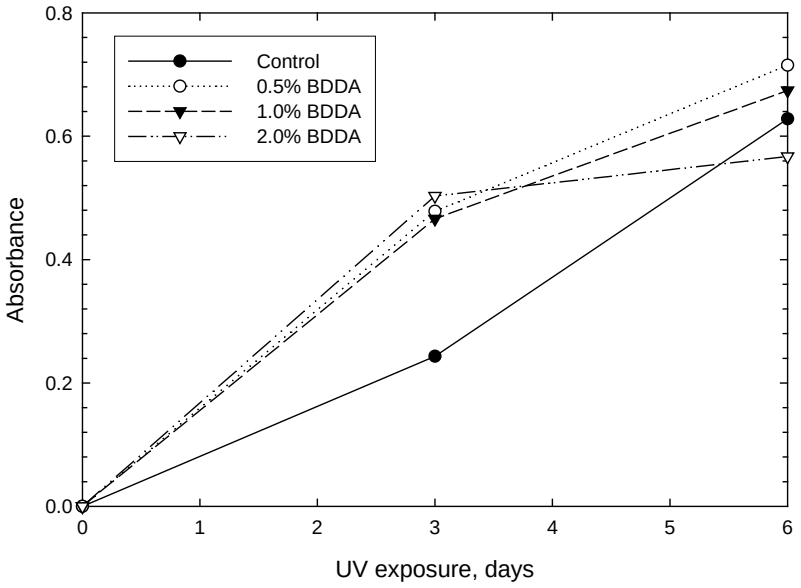

Figure 24. FT-IR absorbance at 1720 cm^{-1} for unmodifed, and BDDA-modified epoxy samples after exposure for 3 and 6 days to UV radiation.

Figure 25. Samples emplaced in styrofoam insulating container.

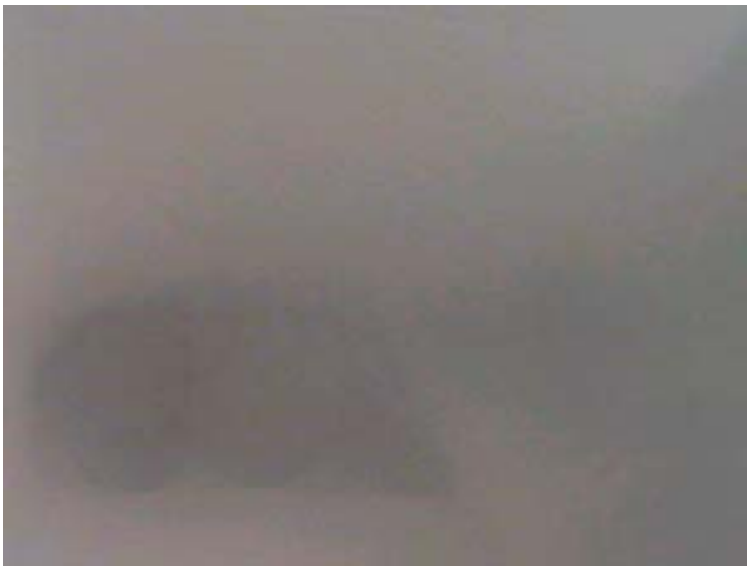

Figure 26. Oxygen deficient vapor cloud that rapidly formed after contact between LN and the warm coating surfaces.

Figure 27. Vapor cloud dispersed after ~ 3 min by air flow.

Figure 28. Samples after being left for 24 hours in air.

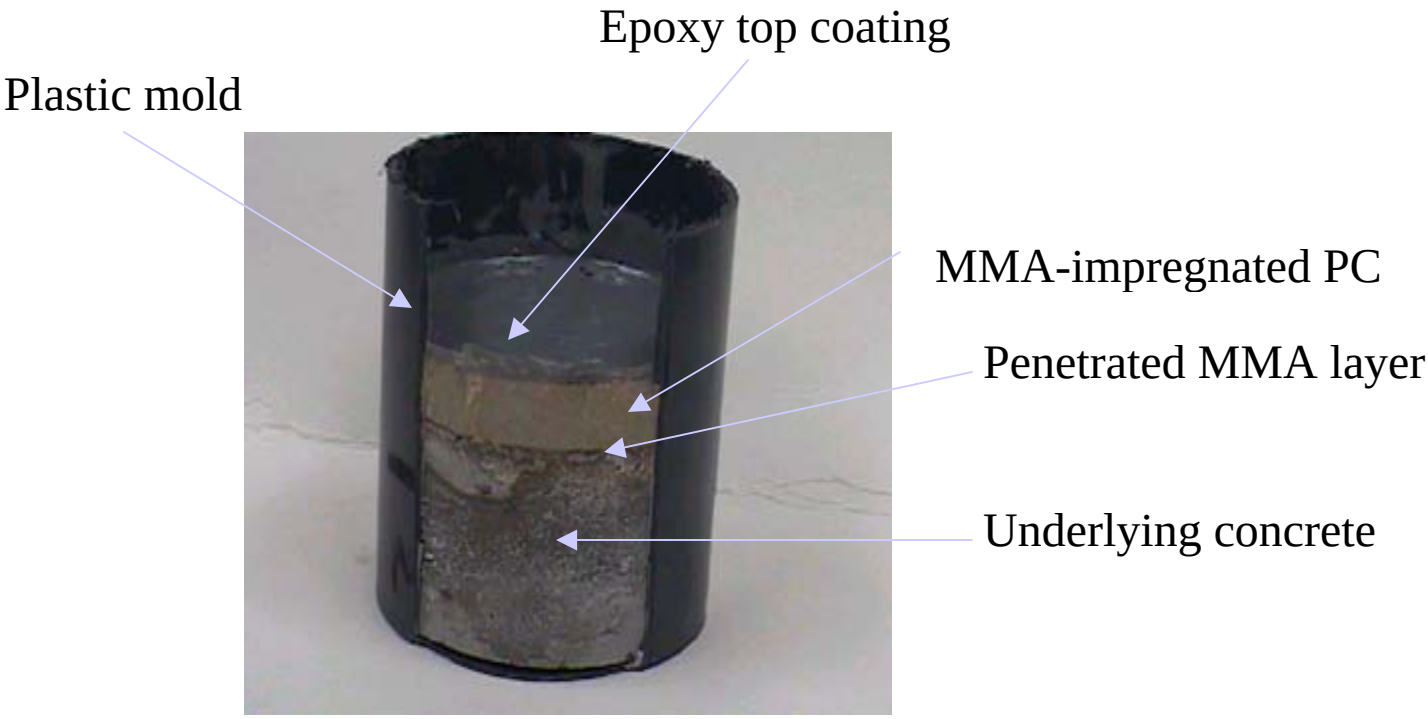

Figure 29. Cross-sectional profiling of repaired PC dike after a spill of LN.

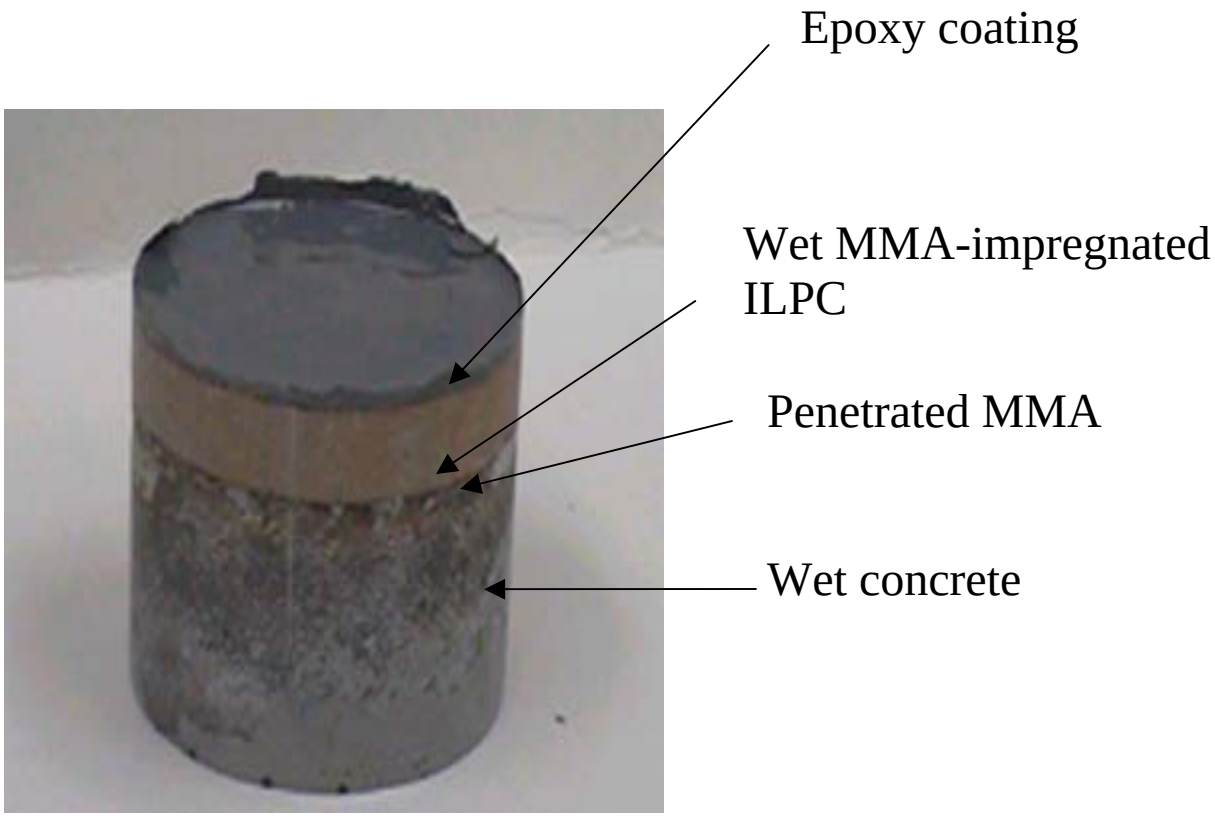

Figure 30. Cross-sectional profile of the wet concrete/penetrated MMA/wet MMA-impregnated ILPC/epoxy coating joint system after 200 freeze-thaw cycles.

Figure 31. Sloped sidewall ILPC test panel located in south side of dike at a LNG facility in Greenpoint, Brooklyn NY.

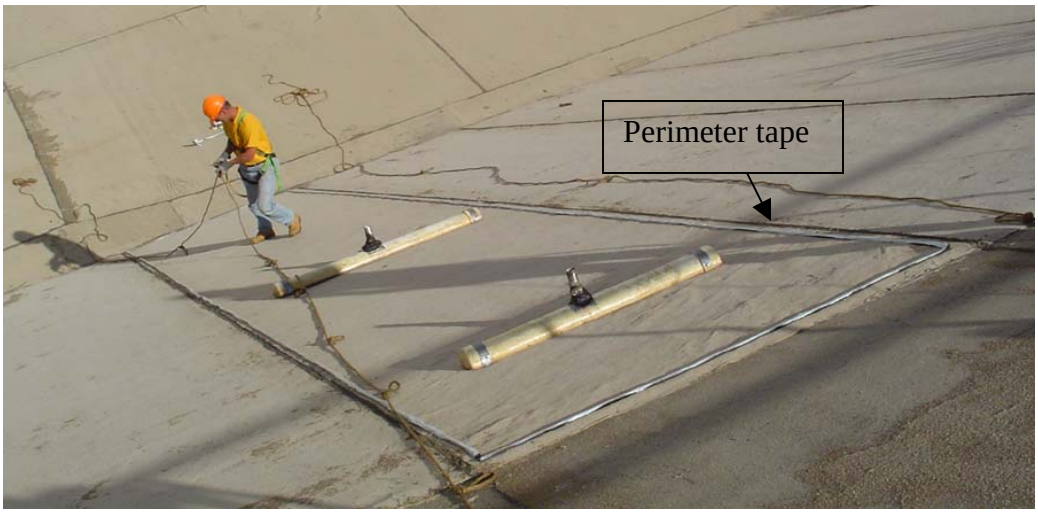

Figure 32. Extremely sticky double-sided perimeter tape adhering to test panel's surface.

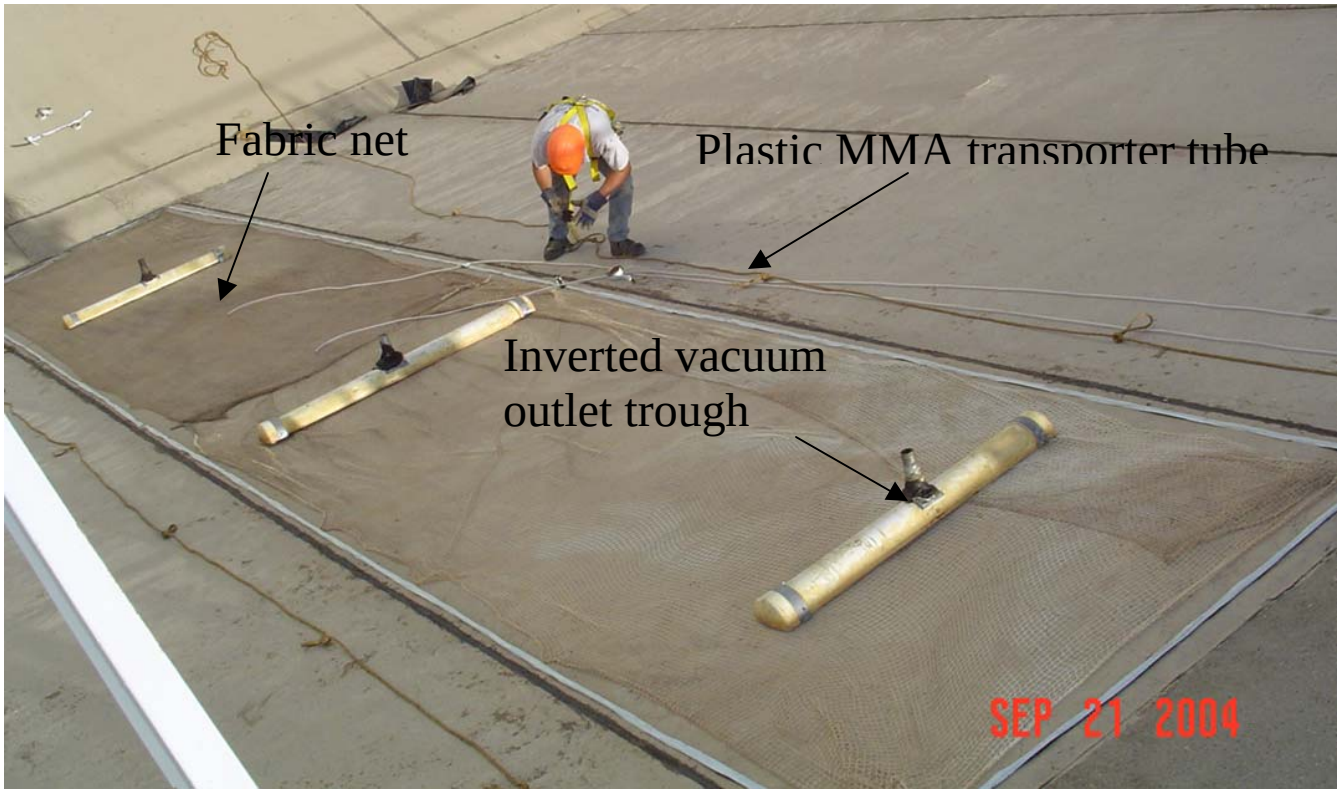

Figure 33. One inch mesh fabric nets were laid down within perimeter tape border. The closed end-inverted troughs attached to 2-in. vacuum outlet pipe nipple were then deployed on fabric nets. The ½ in. inside diam. clear plastic tubes, which transport MMA monomer, were sited in the areas to be impregnated.

Figure 34. Six mil-thick polyethylene sheet was placed over the panel, and then it was pressed to the sticky tape at the perimeter to seal a vacuum-impregnation area.

Figure 35. 2-in. diam. hoses (left) were connected between the pipe nipples that were attached to troughs and the vacuum pump (right).

Figure 36. Polyethylene sheet was immediately sucked down after vacuuming, demonstrating that the perimeter sticky tape had tightly sealed the area (enlarged area, right photo).

Figure 37. BPO catalyst was added to a 5 gallon MMA monomer container.

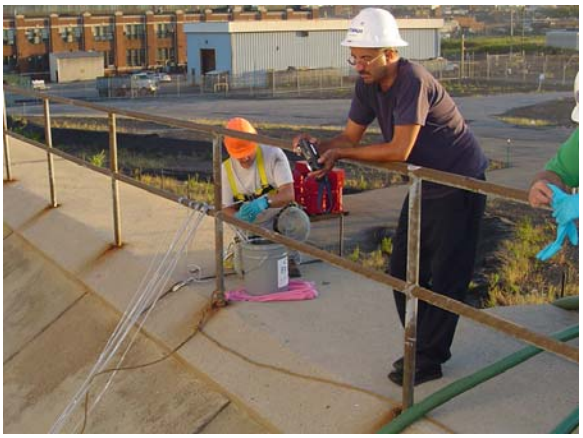

Figure 38. Five clear plastic MMA transporter tubes were immersed in a 5 gallon MMAcontainer.

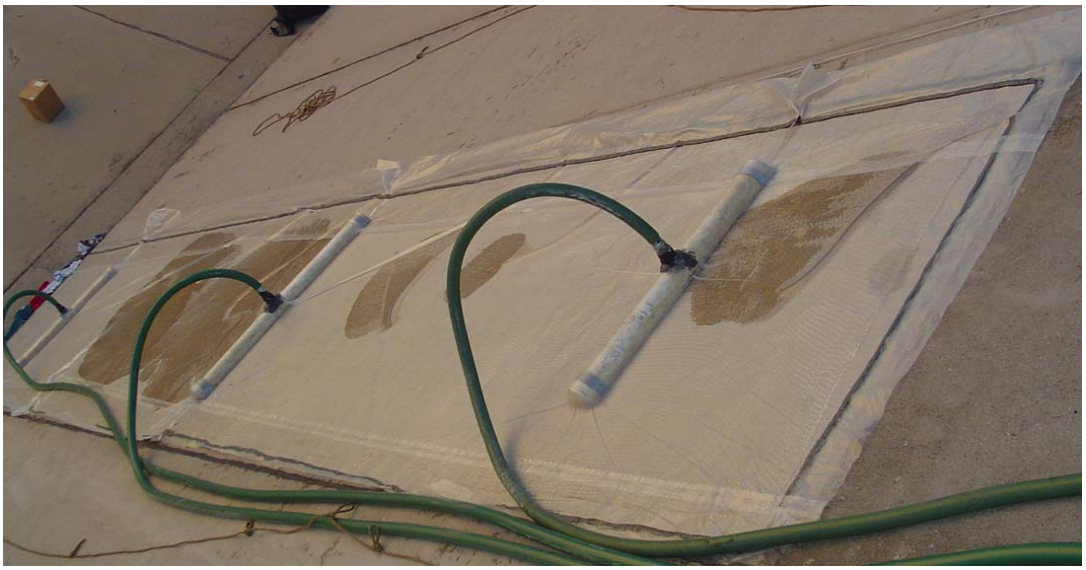

Figure 39. After vacuuming for 40 min, MMA was dispersed on the test panel underneath the polyethylene sheet, while continuously running the vacuum pump.

Figure 40. Vacuuming- MMA impregnation operation of damaged ILPC panel sealed with polyethylene sheet.

Figure 41. After completing MMA impregnation, the vacuum pump was turned off, and the polyethylene sheet peeled off from the adhesive tape.

Figure 42. About 95% of total surface area of panels was wetted by MMA, and ~ 14 gallons of MMA was used in this operation.

Figure 43. Using a roller, the remaining non-wetted portions, representing about 5 %, were covered with additional MMA.

Figure 44. Preparation of epoxy top coating.

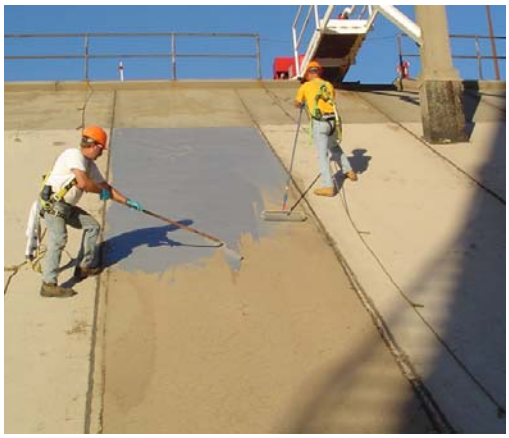

Figure 45. Using 4.5 gallons of epoxy coating, the first layer was applied by roller on the MMA-impregnated ILPC panel.

Figure 46. Three gallons of epoxy were used to fabricate a second coating layer over the first layer.

Figure 47. Comparison of appearance between the repaired (left) and non-repaired (right) ILPC panels.

Figure 48. Collection of a core sample from the repaired ILPC panel with a drilling bit.

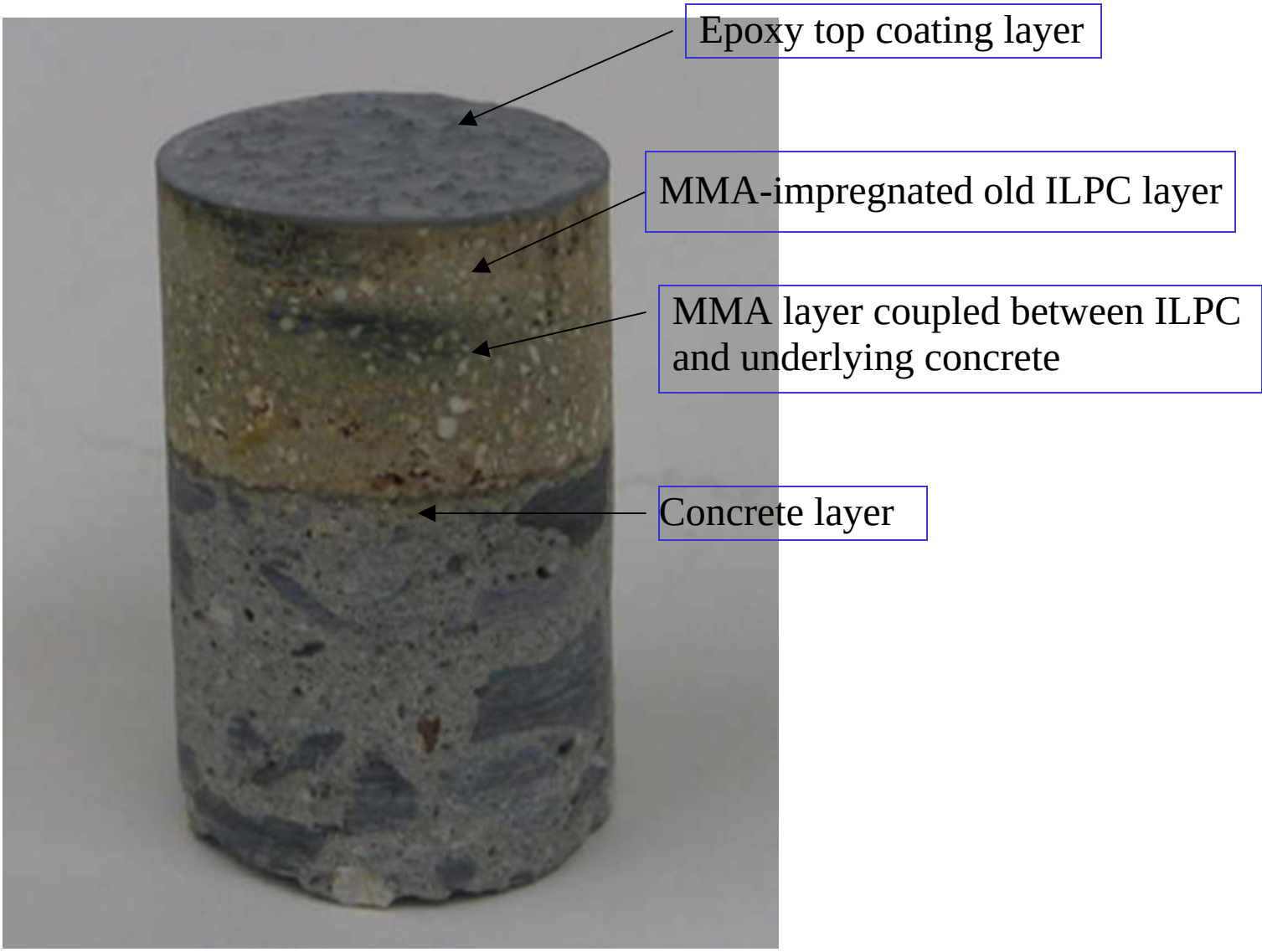

Figure 49. Cross-sectional profile of repaired ILPC core sample.

Figure 50. Core sample of non-repaired ILPC.

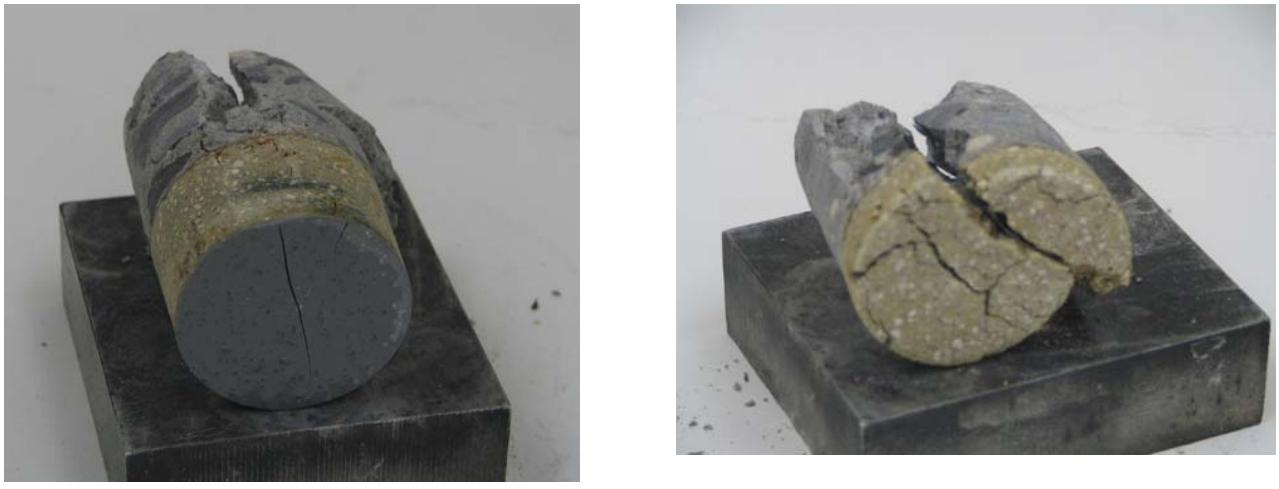

Figure 51. Repaired ILPC (left) and non-repaired ILPC (right) after tensile spread destructive test.

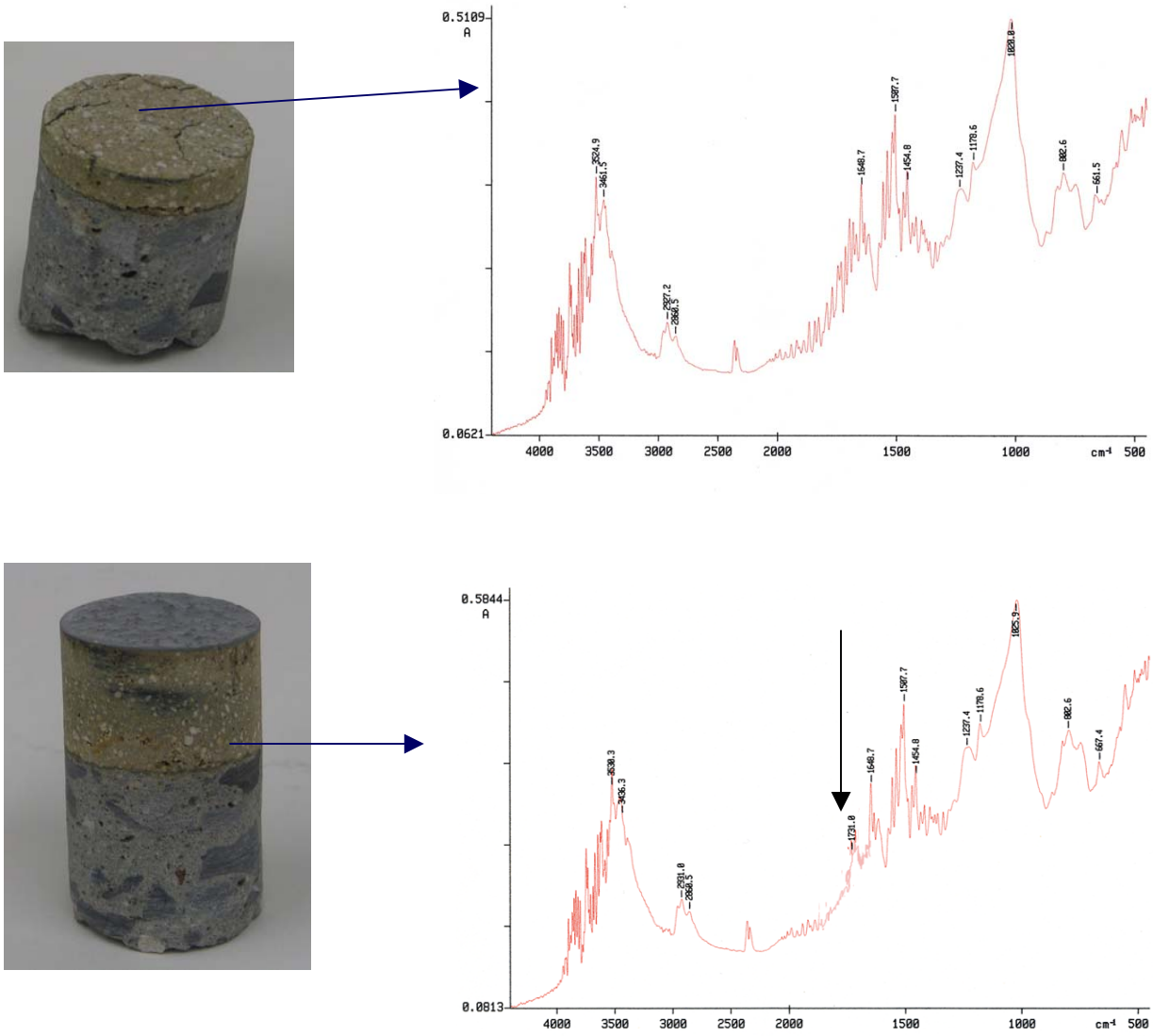

Figure 52. FT-IR spectra for MMA-impregnated (bottom) and non-impregnated (top) old ILPC layers.

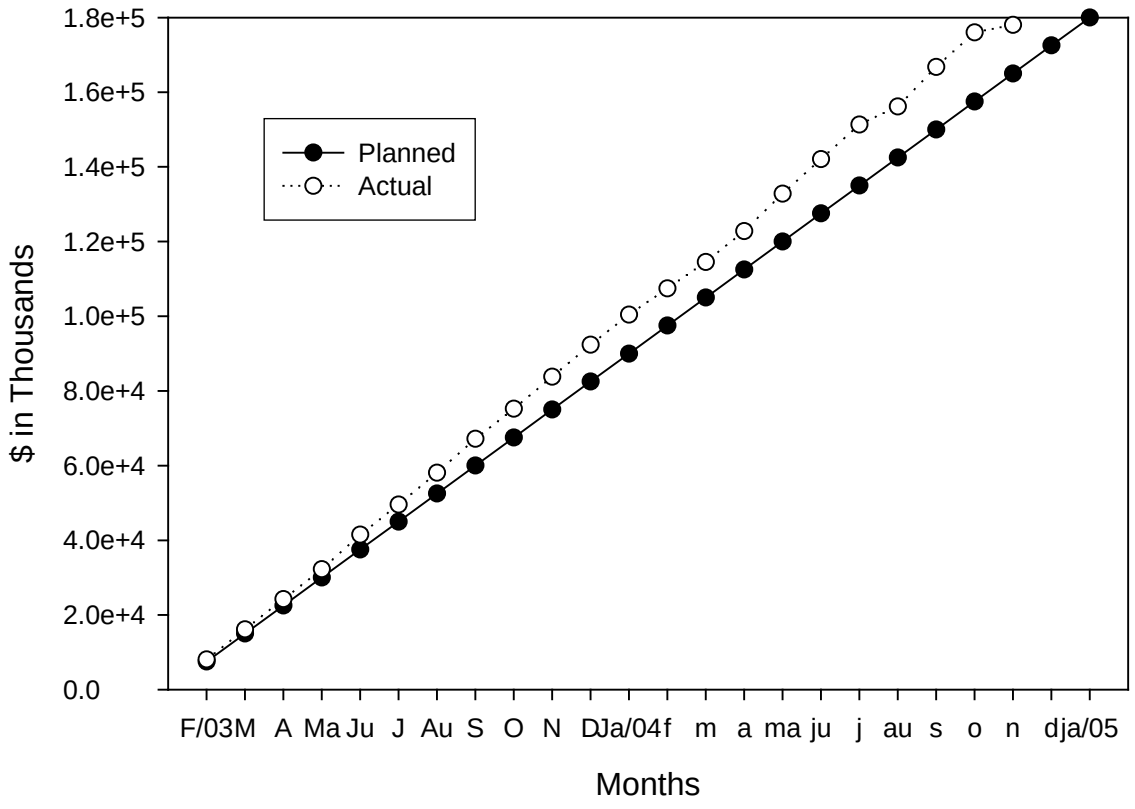

Figure 53. Rate of spending for 2003, 2004, and 2005

Supplemental Work

Almost a year later after the panel was repaired, we visually observed the development of some cracks in the middle location of panel. The failure assessment revealed that although the catalyzed MMA monomer, supplied from Fox Industries Inc. was fully permeated through the damaged ILPC, there was no curing of MMA in this particular area of the panel. Consequently, Balvac Inc. recommended that we evaluate a different-grade MMA made by Chemmasters Corp. to ensure that it cures satisfactorily.

Objective

The objective of this supplemental work was to investigate whether a new MMA system, supplied by Chemmaster Corp. replaces the Fox Industries-made MMA. The factors to be investigated for a new MMA included the curing time as a function of catalyst content and atmospheric temperature, the ability to permeate through a crack's width as small as 0.0025 in. using vacuuming-impregnation sealing technology, and the adherence to wet or dry cement concrete, damaged dike, and epoxy topcoating. Contingent upon the data obtained from this investigation, work to modify the original formula of MMA would be performed to meet the criteria as a water-compatible repairing material. If a damaged dike was repaired successfully by this new MMA, we would conduct the post-field test analyses to interpret the MMA's repairing performance.

Project Schedule and Funding:

This work at a founding level of $24,500 began in August 2005 and was completed in September 2005. It consisted of the following six tasks:

Task A. Setting time of catalyzed MMA at different temperatures.

Task B. Bond strength between MMA and wet or dry substrates.

Task C. Penetration of MMA in cracks of different widths.

Task D. Reformulation (if it is required).

Task E. Report including all information on Tasks A-D.

Task F. Post-test analyses of repaired dike after field demonstration.

Results and Discussion

Task A. Setting Time of Catalyzed MMA at Different Temperatures

The new MMA system consisted of three components, MMA (Duraguard 401, Part A), catalyst (Part C), and promoter (Part B). Table 1 gives the gel time of MMA by varying the amounts of catalyst and promoter at 50° and 77°F.

Table 1.

Temperature, °F	MMA, wt%	Catalyst, wt%	Promoter, wt%	Gel time, min
50	91	6	3	>180
50	88	8	4	172
50	85	10	5	144
50	82	12	6	66
50	79	14	7	21
77	92	5	3	125
77	90	7	3	95
77	88	8	4	62
77	85	10	5	30

Assuming that an appropriate gel time of catalyzed MMA in the total operation process including the mixing and impregnation was around 60 min, the data revealed that two formulations, 82 wt% MMA, 12 wt% catalyst, and 6 wt% promoter and 88 wt% MMA, 8 wt% catalyst, and 4 wt% promoter, can be recommended for use at 50° and 77°F, respectively.

Task B. Bond Strength Between MMA and Wet or Dry substrates

Using these opted formulations, our attention next turned to investigating the adherence of MMA to the surfaces of damaged old PC and cement concrete under wet and dry conditions. The flexure bond strength specimens were prepared in the same manner as employed in evaluating the previous Fox Industries-made MMA. Table 2 shows the test results from bond strength at interfaces between the MMA-impregnated ILPC layer and the concrete.

Table 2.

Temperature, °F	Surface of damaged PC	Surface of concrete	Bond strength, psi	Adhesion failure mode
50	Dry	Dry	69.2	Cohesive failure in concrete
50	Wet	Wet	68.0	Cohesive failure in concrete
77	Dry	Dry	67.5	Cohesive failure in concrete
77	Wet	Wet	68.8	Cohesive failure in concrete

A very encouraging result was obtained from this bond strength test; namely, this MMA had a far better adherent property to ILPC and concrete surfaces than that of the Fox-made MMA. Although their surfaces were wetted, the interfacial bond strength of more than 65 psi was determined, reflecting the cohesive failure mode at which the breakage took place in the concrete.

Task C. Penetration of MMA in Cracks of Different Widths

The final experiment was concentrated on assessing the ability of the formulated MMA to wick and permeate easily into crazed and crack networks as narrow as 0.003 in under vacuuming. Table 3 provides the results from our visual observations of the defective ILPC disk-to-concrete joints after impregnation of MMA at 50° and 77°F.

Table 3.

Temperature, °F	Range of crack's width, in.	Penetration of MMA	Filling activity of MMA in the interstices between ILPC disk and concrete
50	0.003-0.007	Good	Partially filled
50	0.009-0.013	Excellent	Fully filled
50	0.012-0.025	Excellent	Fully filled
77	0.003-0.007	Excellent	Fully filled
77	0.009-0.013	Excellent	Fully filled
77	0.012-0.025	Excellent	Fully filled

The test results showed that the vacuuming-impregnation technology allowed this MMA system to permeate through a fine crack less than 0.004 in. wide, and also to fill the interstices between the ILPC and the underlying concrete. However, at 50°F, we observed that the MMA which permeated through the finest crack range of 0.003-0.007 in. wide did not fully fill in the interstices between ILPC and concrete, seemingly suggesting that the increase in viscosity of MMA at this temperature diminished its ability to infiltrate very fine cracks.

Task D. Reformulation (if it is required)

The integration of all data obtained from the tasks described above suggested that the formula of "as-received" MMA system was adequate to the use as a vacuuming-impregnation repairing material, so that no work to reform its formula was made in this task.

Task F. Post-test Analyses of Repaired Dike after Field Demonstration

Nearly nine months after this new MMA was applied by Balvac Inc. to the damaged dike at the KeySpan LNG facility in Greenpoint, Brooklyn NY, we observed visually the generation of copious map cracks everywhere in the epoxy topcoating layer, and further that some coating layers underwent spallation. To assess why such cracks and spallations occurred, the post-test analyses was focused on two core specimens (size, 3.8 in. in diameter x 3.7 in. in length): One specimen (Figure 54) was taken from the area where the damaged ILPC layer was lifted up by its pronounced delamination from the underlying concrete. The photo images represented the fact that MMA satisfactorily penetrated through the cracks in the ILPC layer and the penetrated MMA was adequately cured. However, a close-examination revealed that the interspaces created by the delamination of the ILPC layer do not fully fill up with MMA, and yet the cured MMA was more likely to be associated with the elastic state, rather than the solid state. One possible cause for this unsatisfied impregnation was due to moisture remaining in the spaces. If this interpretation is valid, the magnitude of the vacuuming applied in the field was not enough to eliminate all the moisture present in the interspaces, and additionally,

there was a necessity of heating the ILPC dikes using a hot air-blowing heater before the vacuum operation. The second core specimen (Figure 55) revealed a great performance of the impregnated MMA in the coupling between the damaged ILPC layer and underlying concrete.

To identify how strongly the impregnated MMA cross-links between the repaired ILPC and concrete, we determined the splitting tensile strength for these core specimens (Figure 56). The test results showed that a well adhered second core specimen (left) had the splitting tensile strength of 342 psi, and the splitting breakage occurred through an entire core specimen, clearly demonstrating that the delaminated ILPC layer was strongly linked by impregnated MMA to the underlying concrete. In contrast, for the first core specimen involving two undesirable factors, a poor filling effect of MMA in the interspaces and a elastic behavior of cured MMA, the feature of its splitting breakage (right) was quite different from that of the second core specimen; the breakage only took place in the underlying concrete, but not the repaired ILPC. This failure mode clearly verified that these undesirable factors weakened a coupling effect of impregnated MMA in cross-linking structure between repaired ILPC and concrete, thereby resulting in ~ 23 % lower splitting tensile strength than that of the second core specimen.

The integration of all the data described above clearly demonstrated that the copious map cracks and spallations of anti-UV and –flammable epoxy topcoating deposited on the repaired ILPC was due to its thermal stresses by heat-cooling fatigue cycles in the field. To deal with this problem, the coatings will be required to posses the following three critical properties: 1) Excellent thermal stability; 2) sufficient elasticity; and, 3) outstanding toughness. In addition, they must be resistant to UV, flame, and spilled LNG at the cryogenic temperature of -160°C (-260°F), and yet be well adherent to the underlying repaired dike.

Conclusions and Recommendations

In the laboratory, this new MMA system proved a potential candidate as a repairing material of damaged old ILPC overlays using vacuuming-impregnation technology. Comparing with that of the Fox Industries-made MMA, one major difference was its very slow curing process, thereby resulting in minimal shrinkage of the cured

MMA. Although no scientific support on the chemistry of “as received” MMA was available, this MMA possessed some water compatibleness. Thus, these two factors, low shrinkage and water compatibility, can be taken as the reason why the adherence of MMA to wet concrete was outstanding. However, one shortcoming of this MMA was a higher viscosity compared with that of Fox’s MMA, raising concerns that the depth of its penetration through the cracks might have a limitation, thereby depending on the degree of vacuum and atmospheric temperature.

Nevertheless, contingent upon the field temperatures, the two formulations, 82 wt% MMA, 12 wt% catalyst, and 6 wt% promoter and 88 wt% MMA, 8 wt% catalyst, and 4 wt% promoter, can be recommended for use in environments at 50° and 77°F, respectively.

Using the former formulation, a field demonstration was performed by Balvac Inc. in October 2005. As a result, significant progress was made from this field demonstration; namely, new MMA allowed it to permeate adequately through the cracks in the damaged ILPC layer, and it was fully cured in the interspaces created by delaminating the ILPC from the underlying concrete. However, although our in-house work revealed that this MMA had some water compatibleness, the presence of an excess amount of water in the interspaces led to the elastic behaviors of cured MMA polymer, causing its poor coupling effects on cross-linking between the repaired ILPC and underlying concrete. Thus, to eliminate any moisture trapped in the interspaces, the surfaces of ILPC layer need to be heated by a hot air-blowing heater before the vacuuming operation.

Another critical issue to be addressed was the failure of the epoxy topcoating that protected the repaired ILPC against UV radiation and fire. The failure assessment showed that the copious map cracks and spallations of the coating layer were due to its thermal stresses by heat-cooling fatigue cycles in atmospheric environments. To deal with this problem, we recommended the development of coatings, which will possess the following three critical properties: 1) Excellent thermal stability; 2) sufficient elasticity; and, 3) outstanding toughness. In addition, there must be resistant to UV, flame, and spilled LNG at the cryogenic temperature of -160°C (-260°F) as well as strong adherence to the underlying repaired dike.

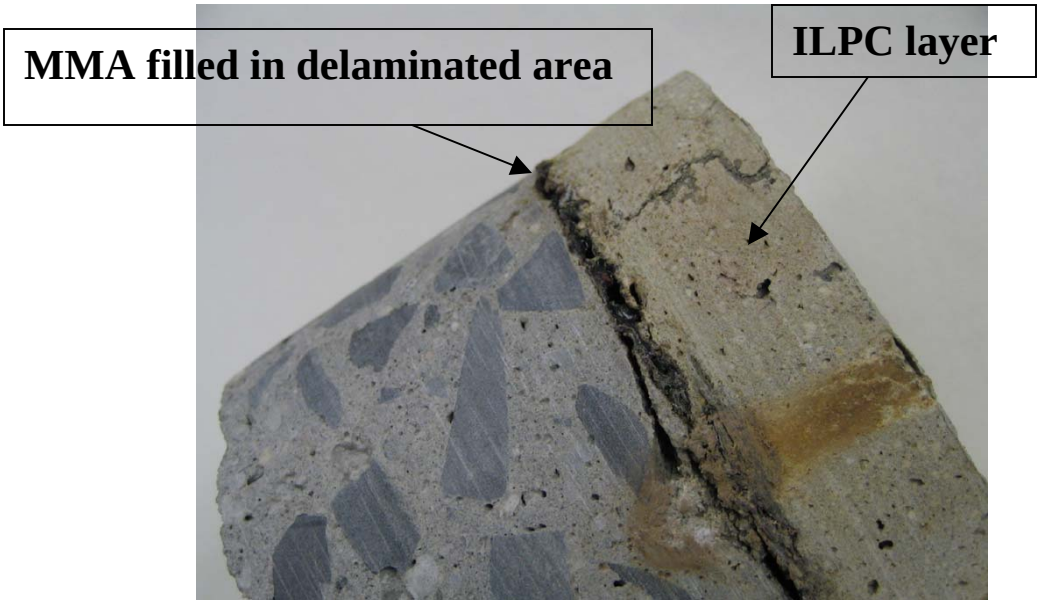

Figure 54. First core specimen taken from the repaired ILPC overlays.

Figure 55. Second core specimen.

Figure 56. Splitting tensile strength test for these core specimens.